Structural assessment of existing R.C. half-joint bridges according to the new Italian guidelines

Structural assessment of existing R.C. half-joint bridges according to the new Italian guidelines

Fabrizio Palmisano[a]*, Rebecca Asso[a], Bernardino Chiaia[a], Giuseppe Carlo Marano[a], Carlo Pellegrino[b]
[a] *DISEG, Politecnico di Torino, Torino, Italy*
[b] *DICEA, University of Padova, Padova, Italy*

** corresponding author: DISEG, Politecnico di Torino, corso Duca degli Abruzzi 24, Torino, Italy, e-mail f.palmisano@ppvconsulting.it*

Abstract:
In 2020, the Italian Guidelines for the classification, assessment and management of bridges were published, introducing a novel multilevel approach to assess the degree of risk of existing bridges at the national scale. Even if these guidelines give, for the first time in Italy, a comprehensive approach to the assessment and management of bridges, in some cases, detailed procedures are missing. One of these cases is represented by the R.C. half-joint, a kind of deck/girder connection that was commonly used in the past. This joint deserves particular attention in the assessment since in many cases it is subjected to deterioration and the relevant reinforcement is not properly designed for the lack of specific provisions in the old Italian technical standards. In this scenario, this article aims to propose a specific methodology for the assessment of half-joints that is consistent with both the above-mentioned Italian Guidelines and the current Italian Technical Standard. However, this methodology can be used as a reference also in other Countries since most of the relevant provisions are general whilst the detailed rules are Eurocode-based. In this article, first the type of investigations to be performed to reach a proper knowledge level is defined, describing possible destructive and non-destructive tests. Then, a procedure for numerical verification of the joint is described. This procedure, based on the adoption of three different Strut-and-Tie Models is introduced and deeply analysed, highlighting the limits and the benefits of each model. Finally, the application of this procedure to a case study is shown.

Keywords: existing bridge, assessment, half-joint, deterioration, Strut-and-Tie model.

1 Introduction

The Italian road network covers about 840,000 km and includes highways (managed by the national agency for roads ANAS or private companies), provincial and municipal roads [1]. The total number of bridges is unknown but according to a first estimate it would be of about 60,000 units. Most of existing bridges were built more than 50 years ago and are concrete structures. Because of lack of inspections and maintenance, many Italian bridges are subjected to significant phenomena of deterioration that in some cases, in addition to hidden structural defects due to design or

construction errors, have triggered catastrophic collapses. It is sufficient to say that in Italy, in the last 10 years, there have been 15 collapses (total or partial), all but one when the bridges were in operation, with a total of 52 fatalities and 38 injured.

The current situation would require in-depth analyses to be carried out on all infrastructures to assess the actual level of safety, according to current national standard, and to define appropriate (construction and/or operational) interventions. However, the large number of infrastructures does not allow to carry out detailed structural assessment on all bridges, thus a stepwise process with increasing level of detail (i.e. multilevel approach) is needed. The multilevel approach makes it possible to start with preliminary and rapid assessments, applicable at territorial scale, in order to select a limited number of bridges that deserve the detailed assessment. This approach is followed by the recent Italian 'Guidelines for risk classification and management, safety assessment and structural health monitoring of existing bridges' [2] (IGB in the following). The approach given in IGB is general and perfectly consistent with the current Italian Technical Standard [3] (ITC in the following). However, there are some cases where the application of IGB needs further detailed procedures that are not defined in the guidelines so far. In this scenario, after a brief description of IGB, this article proposes a new comprehensive methodology for the detailed structural assessment of existing R.C. half-joints that is perfectly consistent with IGB. A numerical example is finally presented to show the completeness of the methodology. Taking into account that most of its provisions are general and that the detailed rules are Eurocode-based, the applicability of the proposed methodology can be considered as not limited to Italy.

It is worth noting that even if in the literature there are many documents on the design of half-joints, very few have been found relevant to the assessment of them and only one [4] gives a general methodology for the assessment. However, differently from what here proposed, the UK guidelines [4] are mainly devoted to the rapid risk assessment of half-joints with few indications on detailed verifications. Conversely, the proposed methodology focuses mainly on specific detailed rules (see e.g. paragraph 4.2) since the general procedure to be used for the rapid risk assessment is included in IGB.

2 The Italian guidelines

The stepwise approach given in IGB is based on six different levels of increasing depth and complexity. The first three levels (i.e. 0-2) should be carried out for all bridges and aim to define, for each bridge, a risk indicator called 'attention class' that combines structural, seismic, geotechnical and hydraulic risks.

Level 0 involves the census of the main characteristics of bridges through the collection of available information and documentation. Level 1 envisages the execution of direct visual inspections and rapid survey aimed to identify the state of deterioration and the main structural and geometric characteristics of bridges, as well as potential risk conditions associated with landslides or hydrodynamic actions. Based on the information gained in Levels 0 and 1, in Level 2 an

attention class is associated to each bridge. To this aim five attention classes are defined in IGB (i.e. low, medium-low, medium, medium-high, high).

For all attention classes, routine inspections are recommended whilst for medium-high and high attention classes the bridge management system should include structural health monitoring.

Level 3 should be carried out in case of medium or medium-high attention class. This level includes a preliminary assessment of the bridge that should be performed by the comparison of the traffic load models given in the current code of practice [3] with those included in the code in force at the time of construction. The aim of level 3 is to understand if a detailed assessment according to ITC (i.e. Level 4) is needed. Level 4 applies also in case of high attention class.

Level 5 should be carried out only for bridges of significant importance within the road network and requires a specific study for the resilience of bridge network which is not covered by the current version of IGB.

In addition to what above mentioned, according to IGB, in case of post-tensioned R.C. bridges and for those placed where there is evidence or knowledge of landslides, flooding or erosional phenomena, detailed inspection (called 'special inspection') should be performed together with Level 4 assessment.

It is worth highlighting that in case of half-joint bridges the application of the IGB approach will often lead to medium-high or high attention class implying the necessity to perform a preliminary or detailed assessment, respectively, even in absence of deterioration or any evidence of structural defects. In this scenario, since neither IGB nor ITC give provisions for the assessment of half-joints, in the following, a methodology for the assessment of these structural elements is proposed. This methodology is consistent with both IGB and ITC and it is Eurocode-based.

3 R.C. half-joint deck structures

A half-joint (also called 'Gerber joint' or dapped-end beam) is a specific type of joint in which the depth of a girder or a deck is significantly reduced at its ends, and it is supported by a similar but mirrored cantilevering element [5] (Fig. 1). It was firstly introduced by Gottfried Gerber, a German engineer who lived in the XIX century, to add an internal hinge in a concrete deck or girder keeping a level-running surface.

In Italy this type of joint has been mainly used from the 1960s till the 1990s. It is not known how many half-joint bridges are in service in Italy but considering only the infrastructures managed by ASPI ('Autostrade Per l'Italia', the major private company for the management of Italian Highways), 244 out of 1811 are R.C. half-joint bridges. This solution is not adopted anymore in Italy mainly because the leakage of water through the joint causes inevitable concrete deterioration and consequent corrosion of reinforcing steel. Moreover, the difficulty in accessing the bearing seat for inspection and maintenance complicates the detection of deterioration mechanisms and their evolution in time.

It is worth highlighting that with reference to the above-mentioned bridge collapses occurred in Italy in the last 10

years, one of them can be directly addressed to the failure of the half-joint (i.e. the Annone overpass on SS. 36; [6]).

There are no specific provisions for half-joints in old Italian technical standards. It follows that in the past, for such structural elements, reference was made to textbooks or construction practice. Specific Italian rules for the design of half-joint have been found by the authors only in the 1974 Italian translation of 'Beton-kalender' [7], a German textbook often used in the past as reference by the most expert Italian practitioners. This book suggests considering the nib as a cantilever and making a bending and shear verification in section 1-1 and 2-2, respectively, of Fig. 2a. The book also proposes to round the corners of the nib and to place inclined reinforcement bars at the corners of the corbels. Moreover, it gives an example of a typical reinforcement layout by referring to a drawing taken from a real case study (Fig. 2b).

It is worth noting that in the past (especially until the 1970s), a specific detailed design of the half-joint was not usually carried out by Italian practitioners, who generally extended to it the approaches used for bending and shear verification of the rest of the deck/girder. Hence, the shear reinforcement necessary for the nib (and that should be concentrated in the nib; see Fig. 2b) was often wrongly distributed over a part of the deck/girder usually as long as the total depth of the deck/girder.

Another issue that has negative consequences on the capacity of old half-joints is related to insufficient anchorage length of the bars. This is due to the lack of specific provisions on bond strength in the Italian Technical Standards up to 1972.

It is worth adding that, differently from Italy, in some Countries the design of half-joints was made in the past by using an approach based on the assumption of specific failure mechanisms. In particular, a diagonal crack was assumed and the reinforcement crossing the crack was assumed to yield. By drawing the polygon of forces, the load that the half-joint could carry was derived by solving the relevant equilibrium equations (Fig. 3). The procedure was repeated for several inclined cracks and it provided an upper-bound solution [8], [9].

4 Assessment of half-joint bridges

The proposed methodology is based on two main steps. In the first step (called 'knowledge'), information about geometry, material characteristics, structural details and current state of the joint should be collected. The second step is relevant to numerical analysis and verification of the joint to define the level of risk according to IGB and ITC.

The methodology is limited to a portion of the girder/deck that includes the half-joint. To define this portion, reference has been made to the definition of the so-called D-regions by Schlaich and co-authors [10]. They made distinction between B-regions ('B' stands for beam or Bernoulli) and D-regions ('D' stands for discontinuity, disturbance, detail). In B-regions the Bernoulli's hypothesis of plane strain distribution is assumed valid. Their internal state of stress is easily derived from the sectional forces (bending and torsional moments, shear and axial forces). In D-regions the strain

distribution is significantly nonlinear; these regions may be due to static discontinuities (e.g. point loads caused by supports or anchorage zones) or to geometrical discontinuities (e.g. frame corners or openings in members) or combination of both (e.g. corbel with point load at a column).

The half-joint is a D-region since it includes both static and geometrical discontinuity. According to the principle of Saint-Venant, the discontinuity region of a half-joint should extend beyond the nib up to a distance l* not lower than the total depth (h) of the girder/deck (Fig. 4). However, the portion of the girder/deck to be assessed should include the resisting mechanism of the half-joint that will be shown in paragraph 4.2. Therefore l* could be longer than what above mentioned and extend up to about three times h (Fig. 4).

4.1 Knowledge

According to ITC, the numerical verifications of an existing structure are performed by using the partial factor format and are based on the identification of the relevant Knowledge Level (KL). ITC and its Commentary [11] define three KLs (i.e. KL1, KL2, KL3). The factors determining the appropriate KL are geometry, structural details, materials. The KL achieved determines the values of the Confidence Factor (CF) to be used in the numerical verifications. CFs equal to 1.35, 1.20, 1.00 are associated to confidence factors KL1, KL2, KL3, respectively. The evaluation of CF is needed to determine the assessment value of material strength f_d to be used in the numerical verifications according to the following equation (IGB):

$$f_d = min\left(\frac{f_m}{CF \cdot \gamma_M}; \frac{f_k}{CF}\right) \quad (1)$$

where

- f_m and f_k are the mean and the characteristic value of material strength, respectively;
- γ_M is the material partial factor.

Thus the ‘knowledge’ step is not only useful to gain information about geometry, material characteristics, structural details and current state of the joint but also to evaluate the CF necessary to determine the assessment values of strength to be used in the numerical verifications.

This step is composed of the following sub-steps:

- analysis of the documentation on design, construction and previous (if any) assessment and interventions;
- geometrical survey of the joint (this includes the definition of reinforcement layout);
- identification of deterioration mechanism(s);
- evaluation of material characteristics;
- evaluation of prestressing.

4.1.1 Reinforcement layout

The layout of reinforcing and prestressing steel can only be partially detected from site inspections, hence the information provided from the original design and construction record are of primary importance. Random investigations with covermeters can be performed to confirm information from design and construction records, together with random removal of concrete cover. When the original design and construction records are not available, it is suggested to perform the so-called 'simulated project' (SP; [11]) referring to codes and good practice of the construction period. The aim of SP is to reconstruct the reinforcement layout in order to limit destructive tests. The reinforcement layout obtained by SP should be checked by using non-destructive tests and slight destructive tests (i.e. removal of concrete cover). However, for half-joints, taking into account what mentioned in paragraph 3 about the absence of specific rules in old codes and manuals, it is very difficult the get reliable results from SP.

Visual inspections are necessary to identify crack patterns, damage and deterioration. To this aim it is worth mentioning that the tests performed by Desnerck and co-authors [12], on several half-joints with induced damage and with various steel layouts, have shown their influence on the half-joint capacity. The part of the half-joint on which special attention should be paid during visual inspections should be identified on the basis of the possible failure mechanisms and the relevant crack pattern. To this aim Fig. 5 shows some typical crack patterns resulting from the experimental program performed by Desnerck and co-authors [13].

In Fig. 5, the reinforcement layout NS-REF is the reference configuration. The remaining layouts are derived from this by removing some reinforcement and in particular:

- in NS-ND the inclined reinforcement is missing;
- in NS-NU the U-shaped bar (vertical) bar in the nib is missing;
- in NS-RS some stirrups are missing.

In the right-hand side column of Fig. 5, the cracks that lead to the joint failure (i.e. critical cracks) are shown in bold. The critical cracks are similar in cases NS-REF, NS-ND, NS-NU and develop horizontally at the upper part and diagonally from the re-entrant corner. Among these three cases, a small difference appears in NS-NU where the inclined critical crack is almost sub-vertical and another critical crack (vertical) is present at the support. In the aforementioned three cases, with reference to the secondary cracks (i.e. non-critical), it is worth highlighting that the inclined ones are more widespread and more extensive in NS-REF. Conversely, with reference to NS-RS, the collapse occurs with a crack pattern typical of a shear failure that develops over the entire depth of the beam with many inclined cracks and with the critical crack (inclined) starting from the lower corner of the joint.

With reference to the evolution of the crack pattern, in general the first crack is the one starting from the re-entrant corner. According to what present in the literature (e.g. [13]), this crack tends to develop for a load level of approximately 20-40% of the ultimate load where the highest values of this percentage are reached when this corner is

rounded or inclined and there is a significant concentration of reinforcement in it (as in NS-REF of Fig. 5). Shortly after the first crack, further cracks parallel to it and close to the re-entrant corner develop. The final crack pattern, as above mentioned, differs according to the reinforcement layout (Fig. 5).

The information given here about possible crack patterns and their evolution can be a useful reference when carrying out inspections. However, it is worth highlighting, that what shown in Fig. 5 and the relevant considerations relate only to the structural behaviour of an originally intact half-joint. It follows that deterioration processes (e.g. reinforcement corrosion) may modify, even significantly, the considerations here reported and, thus, the crack patterns can be different from those included in Fig. 5.

It is worth adding that in a preliminary assessment (i.e. in absence of more detailed investigations), it may be assumed that the presence of isolated cracks not exceeding 0.3 mm in non-prestressed half-joint and not exceeding 0.1 mm in case of prestressed half-joint is representative of a slight damage condition (i.e. associated with serviceability limit conditions; [4]). Conversely, if several cracks of this amplitude are present in the same area or if there is presence of cracks of greater amplitude (even if isolated), it is possible that the half-joint is in a condition closer to the ultimate limit state.

4.1.2 Tests to assess deterioration mechanisms

The evaluation of deterioration mechanisms is of fundamental importance to assess the capacity of the half-joint. Some tests useful to this aim are the following:

- ultrasonic or X-ray tomography to identify local discontinuities;
- carbonation depth measurement;
- chloride penetration measurement;
- electrical resistivity measurement of concrete.
- determination of concrete composition (cementitious matrix) by X-ray diffractometric test or thermogravimetric analysis or chemical analysis (e.g. by X-ray fluorescence investigation);
- semi-quantitative determination of concrete composition (cementitious matrix) by scanning electron microscope.
- determination of aggregate type in concrete by petrographic analysis;
- determination of concrete porosity by MIP (mercury intrusion porosimetry) or equivalent methods;
- determination of chloride and sulphate ions concentration in concrete;
- determination of density and water absorption in concrete;
- determination of reinforcement corrosion rate by galvanostatic pulse method;

- measurement of concrete cover by covermeters.

With reference to the assessment of corrosion depth of reinforcement, it is necessary to evaluate, prior to the definition of the investigation plan, whether the expected corrosion is uniform (i.e. uniform reduction of bar cross-section) or localised ('pitting'). This can be done by identifying general and local environmental conditions (e.g. water percolation) and the possible presence of chlorides (e.g. marine aerosols, water percolation with de-icing salt) which may cause 'pitting' phenomena. Thus, the investigation plan should be oriented to the identification of both the parts subjected to uniform corrosion and those where localised corrosion is possible.

Some tests that are useful to assess reinforcement deterioration with reference to reduction of cross section and bond capacity of the bars are the following:

- dimensional analysis: small localised destructive tests (removal of concrete cover) to perform direct measurement of the bar diameter;
- gravimetric analysis: evaluation of the average equivalent diameter of extracted bars following appropriate removal of any rust layer;
- morphological analysis: evaluation of the presence of ‘pitting’ corrosion in extracted bars by means of liquid penetrants and/or scanning electron microscope;
- determination of the corrosion potential of reinforcement.

4.1.2 Tests to assess concrete strength

Taking into account that the half-joint is a critical zone whose capacity could be seriously compromised by invasive (e.g. destructive) investigations, it is appropriate to use a multilevel approach in the definition of the investigation plan to be used to asses concrete strength. In the first phase of this approach, only non-destructive investigations (e.g. SonReb test) should be carried out in the critical zone, possibly combined with partially destructive tests (e.g. pull-out test, Windsor probe test), while in areas outside the critical one, on the same girder/deck, the same tests carried out in the critical zone combined with destructive investigations will be carried out. In this way, the strength of concrete in the critical region will be determined by correlating the results obtained from the destructive investigations (carried out in non-critical regions) with those derived from non-destructive or partially destructive tests. On the basis of the results of this first investigation phase and preliminary numerical evaluations, the necessity of carrying out limited destructive tests also in the critical zone will be evaluated. In any case, destructive testing in the critical zone should be limited in number.

Some tests useful to assess concrete strength are the following:

- laboratory mechanical tests on samples (cores) extracted from the existing structure (compression, elastic modulus, indirect tensile tests);

- ultrasonic pulse velocity measurement;
- rebound hammer test;
- SonReb test (combination of ultrasonic pulse velocity measurement and rebound hammer test);
- pull-out test;
- Windsor probe test;
- pull-off test;
- resonant frequency test.

The assessment of concrete strength should be performed according to the provisions given in EN 13791:2019 [14].

4.1.3 Tests to assess reinforcement strength

Tests to assess reinforcement strength are, in general, destructive. They are laboratory tests performed on bar samples taken from the existing structure to evaluate at least the ultimate and yield strength.

A multilevel approach should be used with reference to the determination of steel strength as proposed for the assessment of concrete strength. In the first phase of this approach, only non-destructive investigations should be carried out in the critical zone, possibly in combination with small, partially destructive tests (e.g. hardness tests on the bars), while in areas outside the critical one, on the same girder/deck, the same tests carried out in the critical zone combined with destructive investigations will be carried out. Thus, reinforcement strength in the critical region will be determined by correlating the results obtained from destructive investigations (carried out in non-critical regions) with those deriving from non-destructive or partially destructive tests. On the basis of the results of this first investigation phase and preliminary numerical evaluations, the necessity of carrying out limited destructive tests also in the critical zone will be evaluated. In any case, destructive tests in the critical zone must be limited in number.

With reference to bond capacity of reinforcement, it is worth highlighting that reinforcement in existing structures may have geometric characteristics that differ from those required by current technical standards. In this scenario the following approach should be followed:

- In case of ribbed bars, if the relative ribbed area f_R (according to EN 10080:2005 [15]) is not lower than that given in Annex C of Eurocode 2 Part 1-1 [16], anchorage and lap length can be evaluated by using the formulation given in Eurocode 2 Part 1-1 [16] without the necessity to perform specific bond tests.
- In case of ribbed bars, if f_R is lower than that given in Annex C of Eurocode 2 Part 1-1 [16], specific bond test according to Annexes C and D of Eurocode 2 Part 1-1 [16] should be performed to evaluate bond capacity.
- In case of plain bars (square or round section), anchorage and lap length can be evaluated by using the formulation given the last draft of the 2nd generation Eurocode 2 prEN 1992-1-1:2021 [17] without the necessity to perform specific bond tests.

- In case of square twisted bars, anchorage and lap length can be evaluated by using the recent proposal by Cairns and co-authors [18] without the necessity to perform specific bond tests. This proposal is consistent with the reliability-based approach of both Eurocodes and ITC.
- In case of bars different from those above mentioned, specific bond test should be performed or conservative formulations could be used.

For prestressed half-joints, the maximum prestressing force assumed to be applied could be derived from the original design and construction records or, if not available from documented information for the applied prestressing system valid at the time of construction. If the prestressing level is not known, the effect of variation in the prestressing force should be subject to sensitivity analysis. The actual prestressing force may be measured by in-situ testing (i.e. steel de-tensioning test, crossbow method).

4.2 Numerical analysis and verification

4.2.1 General

In the proposed methodology, the numerical analysis and verification of half joints are performed at the ultimate limit state (ULS) by using the Strut-and-Tie Model ([19]; STM in the following) that is recognised to be a practical tool to design and verify D-regions [16].

The STM is a tool of the limit analysis and implies that the structure is designed according to the lower bound theorem of plasticity [10]. It consists of three main components: struts, ties and nodes. The struts carry the compressive forces and the ties are the tension members in the model. Nodes, or nodal areas, represent the points where the struts and ties meet [12].

It is often not necessary a deep knowledge of the STM methodology to find truss models that best fit the regions under study since it is often possible to adapt well known pre-solved examples to the specific case under study. In non-standard cases the development of the 'optimum' truss model can require not only an expert practitioner but also it can be extremely time consuming. This is why many procedures (e.g. Load Path Method [10], optimization criteria), that aim to find the most 'accurate' solution with the minimum 'effort', have been proposed in the last decades [20].

In this scenario a procedure, based on STM, and some reference STMs that can be used to numerically verify the capacity of the half-joints are here given.

Since STM is based on the limit analysis, it requires that materials have sufficient deformation capacity to develop the plastic stress redistributions needed in the element. However, the deformation capacity of concrete is limited and this can also be the case for the reinforcement (due to e.g. material response, slip at laps and anchorages, corrosion). This may consequently compromise the applicability of limit analysis to structural concrete. This topic was investigated by

many researchers and the relevant results are reflected in the following provisions of current codes of practice relevant to the design of new structures [21]:

- The brittleness of concrete in compression for high material resistances is accounted for by reducing the equivalent plastic strength.
- Concrete cracking is accounted for by means of a strength reduction factor considering the state of transversal strains.
- The tensile strength of concrete is neglected for equilibrium. Its effect is only considered with respect to its influence on member stiffness and deformation capacity.
- Minimum reinforcement should be provided to avoid brittle failures and to provide the required deformation capacity of the elements.
- Limits to the inclination of the compression field with respect to ties are included to ensure that the deformation capacity is not exceeded.
- Detailing rules shall be considered consistently (e.g. location of anchorage regions and reinforcement arrangement, minimum and maximum bar spacing and confining reinforcement).

Following these rules, STMs can be applied without significant restrictions for the design of new structures.

For the assessment of existing structures, the definition of relevant STMs differs from how STMs would be used in the design of new structures. Assessors are no able to design and place tensile reinforcement freely and define the relevant STM but have to comply with the provided reinforcement layout of the structure under assessment [12]. In many cases, this is a complex task as many load-carrying mechanisms are possible. Thus, if simple STM solutions do not yield sufficient strength, it is needed to proceed to an optimisation of the STMs to maximise the failure load. This allows avoiding, or at least minimising, the strengthening interventions to be applied to the structure.

Moreover, when dealing with old R.C. structures, it is quite common that some of the above-mentioned rules, included in the codes of practice for the design of new structures, are not fulfilled. One typical case is the presence of significant steel corrosion that limits the deformation capacity and, as said before, may compromise the applicability of the Strut-and-Tie method to the case under study. In general, for this and similar cases, approaches to be used to solve this issue could be:

- To make specific tests to assess the deformation capacity of the element.
- To optimise STM solutions by using e.g. compatibility-based stress fields [22] or incorporating kinematic assumptions during the search for the optimal lower-bound [23].
- To consider an upper-bound solution (by assuming a failure mechanisms) and to check whether a lower-bound solution can be admissible for it. In this approach, the failure load can be obtained by equilibrium of the free-

bodies, allowing derivation of the corresponding forces in the ties and struts [24]. If the strength of one element is not satisfied, the mechanism has to be modified in order to satisfy the yield criteria of all elements.

- To use non-linear analyses.

However, with reference to half-joints, in the following it will be highlighted that in most cases there is no need to use advanced approaches or specific tests to check the applicability of the Strut-and-Tie method to the case under study.

4.2.2 Strut-and-Tie models to be used

In this paragraph the STMs to be used in the proposed methodology in absence of deterioration are illustrated. Further information about how to include deterioration effects in these models will be given in paragraph 4.2.3. The verification of half-joints may be carried out by using a simplified approach in which the effect of the application (and diffusion) of prestressing force is treated separately from that of the application of support reaction. If this approach is used, local verifications related to the application of prestressing should be carried out before those related to the application of reaction. In this case, the reinforcement required to satisfy the verifications related to the application of prestressing cannot be taken into account in the models related to the application of reaction.

It is worth noting that in case of post-tensioning, the application of prestressing can also significantly increase the capacity of the joint. Conversely, in case of pre-tensioning, due to the length of the structural part needed to transfer the prestressing action from the cables to the girder/deck, the effect of prestressing can have little or negligible effect on the capacity of the joint.

The interpretation of structural behaviour of half-joints by using STMs has been widely studied in the past and it is possible to find many solutions in literature, from the first research [9], [10], [25],[26] up to more recent studies [12], [21]. This is why standard STMs present in the literature, with slight changes, can be used in case of assessment without the necessity of advanced approaches as those listed at the end of paragraph 4.2.1. However, these advanced approaches can be used, in addition to standard STMs, to further investigate the capacity of half-joints where needed.

In the proposed methodology, if the effect of prestressing is neglected for the verification of the application of the reaction in the half-joint or in absence of prestressing, the STM approach draws inspiration from what suggested by both Eurocode 2 Part 1-1 [16] and Schlaich & Schäfer [25]. In this scenario, the half-joint verification can be performed by a simplified approach where one or a combination of the two STMs indicated in Figs. 6 and 7 is used. In these figures, struts and ties are indicated with dashed and continuous lines, respectively.

It is worth noting that STMs in Figs. 6 and 7 are slightly different from those present in [16] and [25] and, thus, represent an evolution of these models mainly for the following reasons:

- Differently from the models in [25], those here proposed take account of the horizontal reaction.
- Both models to be combined in the approach given by [16] include the horizontal reaction. These complicates

the relevant combination since include an additional variable (i.e. how the horizontal action should be divided within the two models). This is why, in the proposed approach, the horizontal reaction is included only in one of the two models (i.e. Fig. 6).

Moreover, it is worth adding that all models introduced in this paragraph are a step forward also with respect to those given in the recent UK guidelines [4] since they include the effect of the horizontal reaction.

The position of the forces in the right-hand side section of the models in Figs. 6 and 7 is obtained from the resolution of the relevant B-Region by using the classical theory of beams.

It is worth noting that in some cases, depending on the direction of $R_{A,O}$ and/or its magnitude in relation to the magnitude of $R_{A,V}$, some of the struts in Model A (e.g. 3-5, 5-6 in Fig. 6) may become ties; in these cases, Model A must be slightly modified so that ties are consistent with the reinforcement present.

Vertical and horizontal reinforcement in the nib and in the adjacent area is present only in model A (i.e. ties 3-6, 5-7 and 1-5) whilst inclined reinforcement is included only in model B (i.e. tie 2-7). It follows that, depending on the reinforcement layout, one of the two models or a combination of both can be used. However, it is worth noting that only Model A can bear a horizontal reaction $R_{A,O}$.

Numerical and experimental analyses have shown that inclined reinforcement is very efficient in terms of structural performance even if difficult to place and anchor and that the best performance at service behaviour (i.e. limitation of crack number and width) is achieved when [21]:

$$R_{B,V} \geq 0.5R_V \tag{2}$$

where

$$R_V = R_{A,V} + R_{B,V} \tag{3}$$

In these models, the value of θ_5 should be equal to that assumed for the inclined struts in the shear verifications and therefore should comply with the relevant limits given in ITC (i.e. $1 \leq cot\theta_5 \leq 2.5$). Conversely, the inclination angles of the remaining struts (i.e. θ_1, θ_2, θ_3) should be between 25° and 65° (see [23] and [27]). Different limits for these angles may be assumed if they are adequately justified by numerical analyses and if they take into account both consistency and the consequent strength reduction of struts [17].

It is worth noting that in some cases, depending on the geometry of the half-joint and its reinforcement, it is possible that the position of node 2 in Model B (taking also into account the bending of the inclined bar in the node) is such that the necessary anchorage length of the inclined bar is not guaranteed. In these cases, Model B should change as in Fig. 8 (red lines; node 2 moves to 2'); however, this change is, first, not consistent since it would imply the lowering of the upper chord and, second, not in equilibrium due to the lack of horizontal reinforcement in node 1.

Similarly, it is possible that in some cases the upper end of the inclined bar is not vertically aligned with node 1. This

could happen for geometrical constraint and/or for the necessity to develop a sufficient anchoring length of the inclined bar. In these cases, the upper cord of Model B, would develop too low to satisfy compatibility conditions (red lines in Fig. 9).

In the cases shown in Figs. 8 and 9, it would not be possible to use Model B, so the above-mentioned simplified approach (based on Models A and B) cannot be used and, thus, a new Model C (Fig. 10) is here introduced. It is worth noting that in some cases, depending on the direction of $R_{A,O}$ and/or its magnitude with respect to R_V, some of the struts in Model C (e.g. 3-5, 5-6 in Fig. 10) may become ties; in these cases, Model C must be slightly modified so that ties are consistent with the reinforcement present.

Model C is the natural fusion of Models A and B and differently from similar models present in the literature (e.g. [4], [25] and [21]) takes account of the horizontal reaction.

The limitations of inclination angles mentioned for Models A and B apply to Model C considering that the limits valid for θ_1, θ_2, θ_3 apply also to θ_6 and θ_7. It is worth adding that in Model C the best performance at service behaviour (i.e. limitation of crack number and width) is achieved when the vertical component of the force in the tie 2'-7 is not lower that 50% of R_V [21].

Model C can be used, in place of Models A and B, not only to solve the above-mentioned problems of Model B, but also as an alternative model.

If the half-joint is post-tensioned and the verifications by using Model A plus B or Model C are not satisfied, different models that account for the post-tensioning force can be used.

Very few examples of STMs for post-tensioned half-joints are present in the literature. Most of them are relevant to the application of strut-and-tie method to case studies (e.g. [28]), thus they cannot be used for a general approach. The recent UK guidelines [4] give two different STMs to be used for post-tensioned half joint but these models don't take account of both the horizontal reaction and the presence of inclined reinforcement.

To overcome this issue a new model (i.e. Model C'; Fig. 11) is here proposed. It is obtained from Model C by adding the post-tensioning force. In Model C', the post-tensioning force is applied to both the upper and the lower part of the half-joint and it is assumed that the cross section is completely compressed at the boundary between the D-region and the B-region (i.e. right-hand side of Fig. 11). Model C' is obtained by superimposing Model C on the well-known model for the diffusion of the post-tensioning force in the structural element (i.e. by adding elements 9-2, 9-1, 1-2, 10-5, 10-6). Moreover, nodes 3 and 6 have been slightly moved to the right to fulfil the requirements on the inclination of strut 10-6.

All the considerations (e.g. about the inclination of the struts, the value of the force to be carried by the inclined tie) previously made for Models A, B, C apply also to this model. In some cases, the tie 1-5 of Model C' may be a strut

depending on the direction of $R_{A,O}$ and/or of the magnitude of the post-tensioning force with respect to that of the other acting forces. If the inclined reinforcement represented by tie 2'-7 is not present in the half-joint, the Model C' can be modified by eliminating this tie and replacing struts 1-2' and 2'-3 with a single strut 1-3.

The verifications of struts, ties, nodes of the above-mentioned STMs should be performed according to Eurocode 2 Part 1-1 [16].

4.2.3 Effect of deterioration on the Strut-and-tie Models to be used

Half-joints often exhibit deterioration signs that are mainly caused by water infiltration and stagnation. For example, according to the investigation described in [5] and performed on 219 half-joint bridges, 61.2% of bridges showed cracking defects and 38.4% showed corrosion.

In case of concrete structures affected by deterioration, the assessment should account for the following possible effects:

- reduced concrete section due to delamination and spalling;
- reduction of cross-sectional area and ductility of the reinforcement;
- stress concentration due to localized corrosion (e.g. prestressing steel);
- stress corrosion (e.g. prestressing steel);
- reduced concrete-steel bond;
- loss of mechanical properties of concrete (e.g. sulphate attack, Alkali-Aggregate Reaction and Delayed Ettringite Formation, frost attack, leaching and
- acid attack);
- cracking or expansion of concrete (swelling due to Alkali-Aggregate Reaction and Delayed Ettringite Formation).

The effects of corrosion in hardened concrete differ from those associated with corrosion prior to concreting. Small amounts of corrosion, up to the level required to induce longitudinal cracking, do not cause loss of bond resistance, and can even increase bond strength by a modest degree, particularly where the bar is in a 'poor' bond casting position. At greater levels of corrosion, the residual bond strength is strongly influenced by the degree of confinement provided by secondary reinforcement in the form of links and by the surrounding structure. Transverse pressure from support reactions increases bond. Links play a valuable role in maintaining residual strength of anchorages and lapped joints. The magnitude of the reduction in residual bond strength is highly dependent on the confinement to the bar and is also affected by concrete quality and environment.

Even if there are many scientific studies in the literature relevant to the bond reduction in case of corrosion, very few codes or guidelines include specific prescriptions. The reduction of bond strength for corroded reinforcement can be

assessed by using the table 6.1-4 of fib MC 2010 [29], for plain and ribbed bars, or the CONTECVET Manual [30] for ribbed bars. However, since the prescriptions given in these two documents are the results of preliminary studies, in some cases they give different results for ribbed bars. A new proposal for ribbed bars will be included in the forthcoming fib MC 2020, chapter 20 [31]. This document includes two alternative models. In the first model, the capacity of a lap or anchorage of a corroded bar is provided. In this model the corrosion effect is considered by using the cross-section loss, assumed as uniform along the bond length. This model also includes the effect of confinement given by transversal reinforcement. In the second model, the effect of corrosion is taken into account by using the ARC (i.e. Anchorage in Reinforced Concrete [32]) model that is based on the fib MC 2020 bond-slip model [31], modified to account for corrosion effects.

With reference to specific studies on the effect of deterioration on the capacity of half-joints, the influence of reduction of cross-sectional area and ductility of the reinforcement at the ultimate resistance of half-joints has been recently studied through numerical models by Rosso and co-authors [33], while Quadri & Fujiyama [34] provide information related to the behaviour of half-joints with induced bond deterioration. Desnerck and co-authors [12] have experimentally investigated the effects on STM predictions of some defects due to deterioration. In the Desnerck's tests the effect of corrosion was introduced by reducing the bar cross section, reducing the anchorage length of the inclined bar, introducing localised cracks around some bars, inserting plastic sheet at the end of some reinforcement. The relevant STMs were modified by reducing the bar cross-section to account for steel corrosion and by introducing specific coefficients taken from the literature to reduce concrete strength and bond strength to account for cracking. The STM predictions were lower than the experimentally obtained capacity. However, the underestimation varied significantly within a range of 16–57%. The main conclusion of the article was that current codes and standards, combined with recent findings and guidelines on deterioration effects, led to safe load bearing capacity estimates.

In case of deterioration, the section properties used to assess section resistance should be consistent with those used in the analysis. According to the last draft of the 2nd generation Eurocode 2 prEN 1992-1-1:2021 [17], if P_x is the corrosion penetration depth for homogeneous corrosion (i.e. loss in cross radius of a bar) the following should be considered as possible consequences of reinforcement corrosion:

- Concrete:
  - for $P_x \geq 0.2 - 0.4$ mm, or crack widths ≥ 1 mm, a reduced concrete section may be considered due to spalling ignoring the cover depth around the corroded bars;
  - for low/medium P_x (i.e. $P_x < 0.2 - 0.4$ mm), or crack widths < 1 mm, it may be assumed that the complete concrete section contributes to the resistance with a reduced compressive strength of concrete due to cracking.

- Ordinary reinforcement:
  - for compressed ordinary reinforcement, a reduced reinforcement strength should be considered due to possible bar buckling before the maximum load is reached, if stirrups are heavily corroded (relevant P_x or pits);
  - in shear the possibility of premature failure of stirrups due to pitting corrosion should be considered;
  - for $P_x \geq 0.2 - 0.4$ mm and/or pitting corrosion:
    - a reduction of elongation at maximum stress can be expected and should be considered for the verifications at ULS;
    - a concentration of the active stress at pits should be considered;
  - low/medium P_x (i.e. $P_x < 0.2 - 0.4$ mm) or homogenous corrosion may be assumed not to affect the stress-strain deformation relationships of ordinary reinforcement.

As mentioned in paragraph 4.2.1, one important aspect to remember is that the STM is based on the lower bound theorem of plasticity and hence is only valid when adequate ductility can develop within the structure. As above indicated, according to prEN 1992-1-1:2021 [17], for $P_x \geq 0.2 - 0.4$ mm and/or pitting corrosion a reduction of steel ductility has to be considered; in this case the lower limit of elongation at maximum force (10% quantile) for the use of STMs without the verification of sufficient deformation can be taken as equal to 5%, i.e. that given by both [16] and [17].

On the basis of what above mentioned and taking into account what illustrated in paragraph 4.2.1, in the proposed methodology the STMs of paragraph 4.2.2 and the relevant verifications should be adjusted as follows to account for deterioration:

- For $P_x \geq 0.2 - 0.4$ mm or crack widths ≥ 1 mm:
  - the compressive strength of struts and nodes should be evaluated by using the reduction factors (to account for cracking) given in [16];
  - the cover depth around the corroded bars should be neglected when defining the dimension of struts and nodes;
  - the cover depth around the corroded bars should be neglected when evaluating the anchorage and lap length; to this aim the formulation given by [17] can be used.
- For $P_x < 0.2 - 0.4$ mm) or crack widths < 1 mm:
  - the compressive strength of struts and nodes should be evaluated by using the reduction factors (to account for cracking) given in [16].

- For corroded bars, the strength loss of the bar should be assumed to be proportional to the section loss. To this aim, for uniform corrosion the reduced bar diameter D_r of figure 12a can be assumed whilst for localised corrosion (e.g. pitting corrosion), if d_p is the pith depth, a hemispherical form of the pit can be assumed (see Fig. 12b) as suggested by [35].
- For corroded bars, the bond strength reduction can be assessed by using the models included in fib Model Code 2020 [31] and in fib Model Code 2010 [29] for ribbed and plain bars, respectively.
- For ordinary reinforcement, if $P_x \geq 0.2 - 0.4$ mm and/or in case of pitting corrosion, tests on corroded bars should be performed to evaluate the elongation at maximum force. If it is lower than 5% the applicability of STMs proposed in 4.2.2 should be checked by using e.g. one of the methods proposed at the end of paragraph 4.2.1.

In the proposed methodology, if P_x is measured by calipers, it is suggested to use a calibrated Vernier caliper with resolution of no more than one-twentieth of a millimetre. The procedure given in ACI 364.14T-17 [36] may be useful for measuring by caliper.

For prestressed half-joints, when tendon corrosion is encountered in the assessment, the normal rules for prestressed concrete should be modified by taking into account the following:

- Strands, wires or bars which have suffered sectional loss that has resulted in them being unable to sustain their prestress force should be considered ineffective at that section. The strength of a section at the ultimate limit state should be based on the remaining cross sectional area of the effective strands, wires or bars only.
- Bonded post-tensioning tendons which are ineffective locally can re-anchor and become fully effective elsewhere. Such tendons should be considered in the assessment only if the quality of grouting in the ducts allows anchorage of the design strength of the prestressing steel.
- Where there is evidence of extensive inadequate grouting, the possible re-anchorage of tendons should not be considered in the assessment without further investigation. If the grouting is too poor to allow re-anchorage of tendons, the member should be treated as unbonded and assessed accordingly.

4.3 Example of numerical verification

An example of the verification of a half-joint according to the models proposed in paragraph 4.2 is given in this section. The joint of this example is taken from a real Italian case study to which appropriate modifications have been made in order to better catch the most significant aspects previously described.

4.3.1 Geometry and assessment values of materials

The half-joint is part of a reinforced concrete bridge ‘T’ girder with a total depth of 2.70 m. The bridge was built in the

late 1950s.The dimensions and the main reinforcement (plain round bars) of the half-joint are shown in Figs. 13-15. Spalling of bottom concrete cover is present at the bottom of the half-joint in the zone between the inclined bars and the anchorage of bars in positions 2, 3 and 2a. Moreover, in this zone the bars in positions 2 and 3 have corrosion penetration depth $P_x = 0.3$ mm.

Strength characteristics of the materials were derived from the investigations carried out according to knowledge level KL3 which implies confidence factor CF = 1.

The strength values are:

- characteristic compressive strength of concrete: f_{ck} = 22.7 MPa;
- average compressive strength of concrete: f_{cm} = 31.5 MPa;
- characteristic yield stress of reinforcement: f_{yk} =270 MPa;
- mean yield stress of reinforcement: f_{ym} =295 MPa.

Tensile tests were performed on some samples taken from bars in positions 2 and 3, in a zone of the girder outside the half-joint where corrosion was present. In these tests the measured elongation at maximum force was greater than 10% even for $P_x = 0.2 - 0.4$ mm.

According to ITC and IGB the following partial factors for ultimate limit state verifications should be used:

- concrete: γ_C = 1.5;
- reinforcement: γ_s = 1.15.

According to ITC and IGB the assessing value f_{cd} of concrete strength is

$$f_{cd} = min\left(\alpha_{cc} \cdot \frac{f_{cm}}{CF \cdot \gamma_c}; \alpha_{cc} \cdot \frac{f_{ck}}{CF}\right) \quad (4)$$

where α_{cc} = 0.85 is the coefficient that takes account of long-term effects on the compressive strength and of unfavourable effects resulting from the way the load is applied. Thus, for the half-joint under study f_{cd} = 17.85 MPa.

Similarly, the assessment value of reinforcement yield strength is

$$f_{yd} = \min\left(\frac{f_{ym}}{CF \cdot \gamma_s}; \frac{f_{yk}}{CF}\right) = 256 \text{ MPa} \quad (5)$$

4.3.2 Verifications by using Models A and B

In this paragraph, the verification of the joint under study is performed by using the above-mentioned Models A and B. Firstly deterioration is neglected. Two different approaches can be used for the verification.

The first approach consists of defining the STM, respecting the geometric limitations of the specific case and those indicated in paragraph 4.2.2 (e.g. strut inclination), and carrying out the verifications directly by applying the acting actions. If the verifications are satisfied, this procedure is sufficient. Conversely, if the verifications are not satisfied, the STM is iteratively modified (by trying to improve the capacity of the most heavily stressed members) with the aim of

finding a configuration that satisfies the numerical verifications.

The second approach is aimed to evaluate the capacity (i.e. maximum reaction action that can be carried by the model at the ultimate limit state) which must then be compared with the corresponding demand. Thus, the second approach is generally more time-consuming than the first one since it often requires more iterations.

For this example, the second approach will be used, evaluating the capacity of the half-joint assumed as the maximum vertical reaction that can be born by the joint to the ultimate limit state.

With reference to Model A, the capacity is evaluated in three different cases:

- Case 1: no horizontal reaction.
- Case 2: horizontal reaction acting from right to left equal to 250 kN.
- Case 3: horizontal reaction acting from left to right equal to 250 kN.

The D-region width is assumed equal to that of the beam web (i.e. 32 cm) since the STM develops mainly in the web width.

Figs. 16-18 show Model A for cases 1-3. In these figures geometry (i.e. width for struts and bars for ties), acting force and capacity ratio (CR; i.e. ratio of the acting force to the maximum resistant force) for each element is shown.

According to [16], resistant stress for ties is f_{yd}, whilst resistant stresses for struts are:

$$\sigma_{Rd,max,1} = f_{cd} = 17.85\ MPa \tag{6}$$

$$\sigma_{Rd,max,2} = 0.6 \cdot \left(1 - \frac{f_{ck}\,[MPa]}{250}\right) \cdot f_{cd} = 9.73\ MPa \tag{7}$$

where $\sigma_{Rd,max,1}$ applies to struts with transverse compressive stress or without transverse tension stress and $\sigma_{Rd,max,2}$ applies to struts with transverse tension stress.

According to [16], resistant compressing stresses for nodes are:

$$\sigma_{Rd,max,CCT} = 0.85 \cdot \left(1 - \frac{f_{ck}\,[MPa]}{250}\right) \cdot f_{cd} = 13.79\ MPa \tag{8}$$

$$\sigma_{Rd,max,CTT} = 0.75 \cdot \left(1 - \frac{f_{ck}\,[MPa]}{250}\right) \cdot f_{cd} = 12.17\ MPa \tag{9}$$

where $\sigma_{Rd,max,CCT}$ applies to compression-tension nodes with anchored ties in one direction and $\sigma_{Rd,max,CTT}$ applies to compression-tension nodes with anchored ties in more than one direction.

The following steps have been followed to define the STMs:

(1) Definition of the joint geometry. The length of the D-region is tentatively defined according to what shown in Fig. 4.

(2) Definition of the position of ties 1-5 and 6-8 so that they are barycentric with respect to the corresponding reinforcement.

(3) Application of the load at node 1.

(4) Definition of the position of chord 3-4 so that it is barycentric with respect to the resistant compressive stress resulting from the resolution of the bending verification in section 4-8.

(5) Calculation of forces at nodes 4 and 8 by using equilibrium conditions.

(6) Tentative assumption of the position of tie 3-6 in compliance with the limits on the inclination of strut 1-3.

(7) Tentative assumption of the position of tie 5-7 respecting the limits on the inclination of struts 5-6 and 4-5.

(8) Modification of the D-region length to ensure that the inclination of strut 4-7 is consistent with that assumed for shear verifications.

(9) Verifications of struts, ties and nodes of Model A added to Model B (shown in Fig. 19) assuming strut widths consistent with both the geometry of the D-region and the geometry of the nodes.

(10) Verification of the reinforcement anchorages of Model A added to Model B.

(11) Possible iteration of steps (6) to (10) to determine the capacity of the D-region.

Fig. 19 shows Model B. In this figure the same symbols as those in Model A are used. It is worth noting that for geometrical constraint related to the position of node 2 in Model B, in this model only some of the inclined bars can be activated (see tie 2-7 in Fig. 19).

For struts and ties that are present in both Model A and Model B, the same geometry is assumed to perform the verifications by the summation of the relevant CRs. The verifications are satisfied if the resulting CRs are not greater than one.

It is quite evident that, in this example, the application of Model A and Model B gives a low capacity since, as above mentioned, only part of the inclined reinforcement can be activated. Thus, the necessity to use Model C arises. This is why in this paragraph neither the verifications of nodes and anchorages are performed, nor the effects of deterioration are taken into account.

4.3.3 Verifications by using Model C in absence of deterioration

In this paragraph, the verification of the joint under study is performed by using the above-mentioned Model C and by assessing the capacity of the joint in the same assumptions and in the same three cases defined in the previous paragraph. In this paragraph deterioration is neglected since it will be considered in pargraph 4.3.4.

Figs. 20-22 show Model C for cases 1-3.

The following steps have been followed to define the STMs:

(1) Definition of the joint geometry. The length of the D-region is tentatively defined according to what shown in Fig. 4.

(2) Definition of the position of ties 1-5, 6-8 and 2'-7 so that they are barycentric with respect to the corresponding reinforcement.

(3) Application of the load at node 1.

(4) Definition of the position of chord 3-4 so that it is barycentric with respect to the resistant compressive stress resulting from the resolution of the bending verification in section 4-8.

(5) Calculation of forces at nodes 4 and 8 by using equilibrium conditions.

(6) Tentative assumption of the position of tie 3-6 in compliance with the limits on the inclination of strut 1-3.

(7) Tentative assumption of the position of tie 5-7 respecting the limits on the inclination of struts 5-6 and 4-5.

(8) Modification of the D-region length to ensure that the inclination of strut 4-7 is consistent with that assumed for shear verifications.

(9) Tentative assumption of the inclination of struts 1-2' and 2'-3 in compliance with the limits on the inclination of struts.

(10) Verifications of struts, ties and nodes assuming strut widths consistent with both the geometry of the D-region and the geometry of the nodes.

(11) Verification of the reinforcement anchorages.

(12) Possible iteration of steps (6) to (9) to determine the capacity of the D-region.

Node 1 of Fig. 22 has no anchored ties, thus, according to [16], its resistant compressing stress is:

$$\sigma_{Rd,max,CCC} = \left(1 - \frac{f_{ck}\,[MPa]}{250}\right) \cdot f_{cd} = 16.22\ MPa \tag{10}$$

It is worth noting that the capacity of the models in Figs. 20-22 depends on the verification of tie 3-6. Moreover, in the model of Fig. 20, the tie 1-5 is not stressed since it is perpendicular to 1-2' and there is no horizontal reaction at the support.

The comparison of Figs. 21 and 22 with Fig. 20 shows that, in this case, the horizontal reaction at the support does not significantly change the capacity of the joint.

There is no need to perform compression verifications for the nodes in Figs. 20-22 since all struts have constant cross section and their CRs are such that the relevant stresses are always lower than the corresponding maximum stresses for the joint verification. The only exception could be strut 3-4 where in the worst condition (i.e. case 1; Fig. 20) the relevant stress $\sigma_{3-4,case\ 1}$ seems to be greater than the resistant stress at nodes 3 and 4:

$$\sigma_{3-4,case\ 1} = \frac{699.6\ \text{kN}}{0.32\ m \cdot 0.14\ m} = 15616\ kPa = 15.62\ MPa > \sigma_{Rd,max,CCT} = 13.79\ MPa \tag{11}$$

However, nodes 3 and 4 are in the upper flange of the girder and the assumption of their width equal to the web width (i.e. 32 cm) is very conservative. In this case a sufficient to assume 37 cm as width of the top chord to satisfy the verification of nodes 3 and 4. This width corresponds to a horizontal stress diffusion in the upper flange of only 2.5 cm per side that is acceptable and on the safe side.

The comparison of the results of Model C (Figs. 20-22) with those of Model A added to Model B (Figs. 16-19)

highlights that Model C, thanks to the possibility to activate the entire inclined reinforcement guarantees the highest capacity of the joint.

In the following, for the sake of the example, only the anchorage verification of $\phi 24$ bars of tie 1-5 in node 5 of case 2 (Fig. 21) is shown. Neither in ITC nor in the current version of Eurocode 2 [16] specific provision for the anchorage of plain bars are given, this is why in the following reference is made to what included in the last draft of the 2nd generation Eurocode 2 [17] that is based on the recent proposal by Palmisano and co-authors [37].

According to [17], the assessment value of the anchorage length of plain bars l_{bd} is given by

$$\left(\frac{l_{bd}}{\phi}\right) = (130 \cdot \eta_1) \cdot \left(\frac{\gamma_C}{1.5}\right)^{\frac{3}{2}\eta_2} \cdot \left(\frac{\sigma_{sd}\,[MPa]}{435MPa}\right)^{\frac{5}{4}\eta_3} \cdot \left(\frac{25MPa}{f_{ck}\,[MPa]}\right)^{\frac{2}{3}\eta_4} \cdot \left(\frac{1.5\cdot\phi}{c_d}\right) \quad (12)$$

where:

- ϕ is the bar diameter;
- σ_{sd} is the assessment value of the stress in the bar that should be not greater than 300 Mpa for the applicability of this formulation;
- c_d is the assessment value of concrete cover equal to the minimum between lateral cover, top/bottom cover, half of net spacing between adjacent bars;
- $\eta_1 = \eta_2 = \eta_3 = \eta_4 = 1$ for good bond conditions according to [17];
- $\eta_1 = 3.1, \eta_2 = 1.6, \eta_3 = 0.9, \eta_4 = 3/5$ for other bond conditions;
- the ratio $\frac{1.5\cdot\phi}{c_d}$ should not be taken lower than 0.5;
- $\frac{l_{bd}}{\phi}$ should be not lower than 10 for the applicability of this formulation.

Equation (12) is valid if $\frac{c_d}{\phi} \geq 1$ otherwise [17] provides the relevant correction coefficients.

According to [17], in case of plain bars with hooks, l_{bd} should be evaluated ignoring the length of the hook but substituting σ_{sd} in equation (12) by the following σ'_{sd}:

$$\sigma'_{sd} = \sigma_{\mathrm{sd}} - \Delta\sigma_{\mathrm{sd}} \geq 0 \quad (13)$$

where

- $\Delta\sigma_{\mathrm{sd}} = 38 \cdot \delta_1 \cdot \left(\frac{\gamma_{\mathrm{c}}}{1.5}\right)^{-\delta_2} \cdot \left(\frac{f_{\mathrm{ck}}\,[MPa]}{25}\right)^{\frac{1}{2}} \cdot \left(\frac{c_{\mathrm{d}}}{\phi}\right)^{\frac{1}{4}}$ (14)
- the ratio $\frac{c_d}{\phi}$ should be limited to 3.0;
- $\delta_1 = \delta_2 = 1.0$ for good bond conditions according to [17];
- $\delta_1 = 0.3$ e $\delta_2 = 2.0$ for other bond conditions.

According to [17], equation (12) can be applied on the condition that the mandrel diameter of the hook is not lower than the minimum value included in the standard in force during the original design and that the straight part of the hook is

not shorter than 5 times the bar diameter. For the bars under study these provisions are satisfied with the clarification that no limits to the mandrel diameter are applicable since there were no specific provisions on the mandrel diameter in the Italian technical standards in force during the original design.

The bars under study ($\phi 24$ bars of tie 1-5 in node 5 of Fig. 21) are in good bond conditions, c_{d} = 2.4 cm (i.e. half of net spacing between adjacent bars), σ_{sd} = 177 MPa; thus from equations (13) and (14) it results:

$\Delta\sigma_{sd}$ = 36 MPa;

σ'_{sd} = 139 MPa;

l_{bd} = 122 cm.

The anchorage verification is satisfied since the provided length is equal to 129 cm thus greater than that required (i.e. 122 cm).

4.3.4 Verifications by using Model C considering the effect of deterioration

In this paragraph, the verification of the joint under study performed in paragraph 4.3.3 by using Model C is adjusted to account for deterioration.

As mentioned in paragraph 4.3.1, in the case under study deterioration is present only at the bottom of the half-joint in the zone between the inclined bars and the anchorage of bars in position 2, 3 and 2a. It consists of the following:

(i) spalling of bottom concrete cover;

(ii) the bars in positions 2 and 3 have corrosion penetration depth $P_{\mathrm{x}} = 0.3$ mm.

As indicated in paragraph 4.3.1, tensile tests performed on some samples taken from bars in positions 2 and 3, have shown that the elongation at maximum force of these samples was always greater than 10% even for $P_{\mathrm{x}} = 0.2 - 0.4$ mm. Since the elongation at maximum force is greater that 5%, according to what mentioned in paragraph 4.2.3, standard STMs, as Model C, can be used. Thus, Models in Figs. 20-22 can be used and should be modified to account for deterioration.

According to what proposed in paragraph 4.2.3 and taking into account the reinforcement layout (see Figs. 14 and 15), in this case deterioration affects only the resistance of tie 6-7 (see Figs. 20-22). The sound cross section of tie 6-7 is equal to 3221 mm^2 while its reduced cross section (evaluated by assuming $P_{\mathrm{x}} = 0.3$ mm for bars in positions 2 and 3) is equal to 2317 mm^2. Thus, the capacity ratio of tie 6-7 in Figs. 20-22 (equal to 0.43 in absence of deterioration) becomes 0.60. This means that the verification of tie 6-7 is satisfied even in case of deterioration and that the capacity of the half-joint is not reduced by the effect of deterioration.

5 Concluding remarks

Half-joints are structural elements commonly used in R.C. bridges built in Italy during the 1960s-1990s. They are easily

susceptible to water infiltrations, which leads to an acceleration of deterioration rate, and often difficult to inspect. Their geometry and static condition make them a typical example of D-regions [10], where beam theory is not valid and structural analysis and verification should be performed by other methods such as the Strut-and-Tie Model [19].

In this article a novel and comprehensive methodology for the assessment of R.C. half-joints has been proposed. This methodology is consistent with the Italian technical standard and the recent multilevel approach included in the Italian 'Guidelines for risk classification and management, safety assessment and structural health monitoring of existing bridges'. Moreover, considering that most of its provisions are general and that the detailed rules are Eurocode-based, the applicability of the proposed methodology can be considered as not limited to Italy.

The proposed methodology is mainly composed of two parts: the first is devoted to the investigations (e.g. inspections, testing) needed to reach a proper knowledge level of the current state of the element, whilst the second is relevant to the numerical verification at the ultimate limit state by using three different Strut-and-Tie Models. The central role played by the knowledge in the assessment of half-joints has been examined, from the importance of visual inspections to the description of destructive and non-destructive tests that can be carried on these elements.

The models proposed for the verification have been critically analysed, also by using a case study as example, in order to give a procedure that can be easily used by practitioners.

References

[1] Cosenza E, Losanno D (2021). Assessment of existing reinforced-concrete bridges under road-traffic loads according to the new Italian guidelines. Structural Concrete 22(5): 2868-2881. https://doi.org/10.1002/suco.202100147.

[2] Italian High Council of Public Works (2020). Linee guida per la classificazione e gestione del rischio, la valutazione della sicurezza ed il monitoraggio dei ponti esistenti (in Italian). Italy.

[3] Italian Ministry of Infrastructures and Transportations (2018). Aggiornamento delle Norme Tecniche per le Costruzioni (in Italian). Italy.

[4] CS 466, Risk management and structural assessment of concrete half-joint deck structures, Revision 0. Highways England, UK, March 2020.

[5] Desnerck P, Lees JM, Valerio P, Loudon N, Morley CT (2018). Inspection of RC half-joint bridges in England: analysis of current practice. Proceedings of the Institution of Civil Engineers – Bridge Engineering, 171(4):209-302. https://doi.org/10.1680/jbren.18.00004.

[6] di Prisco M, Colombo M, Martinelli P, Coronelli D (2020). The technical causes of the collapse of Annone overpass on SS.36. In: di Prisco M & Menegotto M (eds) Proceedings of Italian Concrete Days 2018, Springer Cham, Switzerland: 16 pages.

[7] Manuale del calcestruzzo semplice ed armato (Beton-kalender), volume terzo (1974). C.E.L.I., Bologna, Italy (In Italian).

[8] Reynolds GC (1969). The Strength of Half-Joints in Reinforced Concrete Beams. Cement and Concrete Association, UK.

[9] Mattock AH, Chan TC (1979). Design and Behavior of Dapped-End Beams. PCI journal: 28-45.

[10] Schlaich J, Schäfer K, Jennewein M (1987). Towards a consistent design of structural concrete. PCI Journal, 32(3): 74-150. https://doi.org/10.15554/pcij.05011987.74.150.

[11] Italian Ministry of Infrastructures and Transportations (2019). Circolare 21 gennaio 2019, n. 7 C.S.LL.PP. Istruzioni per l'applicazione dell'«Aggiornamento delle "Norme tecniche per le costruzioni"» di cui al decreto ministeriale 17 gennaio 2018 (in Italian). Italy.

[12] Desnerck P, Lees JM, Morley CT (2018). Strut-and-tie models for deteriorated reinforced concrete half-joints. Engineering Structures, 161: 41-54. https://doi.org/10.1016/j.eng-struct.2018.01.013.

[13] Desnerck P, Lees JM, Morley CT (2016). Impact of the reinforcement layout on the load capacity of reinforced concrete half-joints. Engineering Structures 127: 227-239. http://dx.doi.org/10.1016/j.engstruct.2016.08.061.

[14] EN 13791:2019, Assessment of in-situ compressive strength in structures and pre-cast concrete components. CEN, Brussels, Belgium, August 2019.

[15] EN 10080:2005, Steel for the reinforcement of concrete — Weldable reinforcing steel — General. CEN, Brussels, Belgium, May 2019.

[16] EN 1992-1-1:2004/A1, Eurocode 2: Design of concrete structures - Part 1-1: General rules and rules for buildings. CEN, Brussels, Belgium, December 2014.

[17] prEN 1992-1-1:2021, Eurocode 2: Design of concrete structures - Part 1-1: General rules - Rules for buildings, bridges and civil engineering structures. CEN, Brussels, Belgium, September 2021, document CEN/TC 250/SC 2 N 1896.

[18] Cairns J, Feldman L, Palmisano F (2021). Anchorage and lap capacity of square twisted reinforcement for assessment of existing structures. Structural Concrete 22(5): 2813-2828. https://doi.org/10.1002/suco.202100105.

[19] Ritter W (1899). Die Bauweise Hennebique (in German). Schweizerische Bauzeitung, 7 (33): 59-61.

[20] Mezzina M, Palmisano F, Raffaele D (2012). Designing simply supported R.C. bridge decks subjected to in-plane actions: Strut-and-Tie Model approach. Journal of Earthquake Engineering, 16 (4): 496-514. https://doi.org/10.1080/13632469.2011.653866.

[21] fib Bulletin No. 100. Design and assessment with strut-and-tie models and stress fields: from simple calculations to detailed numerical analysis. State-of-the-art report. Fib, Lausanne, Switzerland, September 2021.

[22] Kaufmann W, Mata-Falcón J, Webe M, Galkovski T, Tran, Kabelac J, Konecny M, Navrátil J, Cihal M, Komarkova P (2020). Compatible Stress Field Design of Structural Concrete: Principles and Validation. ETH Zurich and IDEA StatiCa s.r.o, Switzerland.

[23] Muttoni A, Schwartz J, Thürlimann B (1997). Design of Concrete Structures with Stress Fields. Birkauser, Switzerland.

[24] Muttoni A, Fernández Ruiz M, Niketić F (2015). Design versus assessment of concrete structures using stress fields and strut-and-tie models. ACI Structural Journal, 112(5): 605-615. https://doi.org/10.14359/51687710.

[25] Schlaich J, Schäfer K (1991). Design and detailing of structural concrete using strut-and-tie models. Structural Engineer, 69(6): 113-125.

[26] Barton DL, Anderson RB, Bouadi A, Jirsa JO, Breen JE (1991). An investigation of strut-and-tie models for dapped beam details. University of Texas at Austin - Center for Transportation Research (CTR), Texas, USA.

[27] ACI 318-19, Building Code Requirements for Structural Concrete. American Concrete Institute, 2019.

[28] Reineck K-H, Novak LC (2010). SP-273: Further Examples for the Design of Structural Concrete with Strut-and-Tie Models. American Concrete institute, USA.

[29] fib Model Code for Concrete Structures 2010. Ernst & Sohn, Germany, 2013.

[30] CONTECVET. A validated users manual for assessing the residual service life of concrete structures. Manual for assessing corrosion-affected concrete structures. EC Innovation Programme IN30902I, preparation of document led by Geocisa and Torroja Institute, 2000.

[31] fib T.G. 2.5, Model Code 2020, chapter 20, Bond of embedded steel reinforcement, TS V6 (draft), June 2022.

[32] Blomfors M, Zandi K, Lundgren K, Coronelli D (2018). Engineering bond model for corroded reinforcement. Engineering Structures, 156: 394-410. http://dx.doi.org/10.1016/j.engstruct.2017.11.030.

[33] Rosso MM, Asso R, Aloisio A, Di Benedetto M, Cucuzza R, Greco R (2022). Corrosion Effects on the Capacity and Ductility of Concrete Half-Joint Bridges. Available at SSRN: https://ssrn.com/abstract=4160407 (consulted on the 6th September 2022). http://dx.doi.org/10.2139/ssrn.4160407.

[34] Quadri AI, Fujiyama C (2021). Response of reinforced concrete dapped-end beams exhibiting bond deterioration subjected to static and cyclic loading. Journal of Advanced Concrete Technology, 19(5): 536-554. http://doi.org/10.3151/jact.19.536.

[35] Val D, Stewart M, Melchers R (1998). Effect of reinforcement corrosion on reliability of highway bridges. Engineering Structures, 20(11): 1010-1019. http://dx.doi.org/10.1016/S0141-0296(97)00197-1.

[36] ACI 354.14T-17, Section loss determination of damaged or corroded reinforcing steel bar. American Concrete Institute, 2017.

[37] Palmisano F, Greco R, Biasi M, Tondolo F, Cairns J (2020). Anchorage and laps of plain surface bars in R.C. structures. Engineering Structures, 213: https://doi.org/10.1016/j.engstruct.2020.110603.

Figure captions

Fig. 1 Half-joint beam (a) and relevant detail (b).
Fig. 2 (a) verification sections and (b) typical reinforcement layout of a half joint according to [7].
Fig. 3 Design of half-joint on the assumption of failure mechanisms: (a) location of the diagonal cracks and (b) forces that are acting on the free body.
Fig. 4 Extension of the portion of the girder/deck subjected to the proposed methodology of assessment.
Fig. 5 Reinforcement layout and relevant final crack pattern for some typical cases (after [13]).
Fig. 6 Model A.
Fig. 7 Model B.
Fig. 8 Change (red lines) of Model B when the position of node 2 does not guarantee the needed anchorage length of the inclined bars.
Fig. 9 Change (red lines) of Model B when the upper end of the inclined bar is not vertically aligned with node 1.
Fig. 10 Model C.
Fig. 11 Model C'.
Fig. 12 Residual cross section after corrosion for (a) uniform corrosion and (b) localised corrosion.
Fig. 13 Cross section and lateral view of the half-joint under study (units: cm).
Fig. 14 Cross section (a) and detail of the bottom part (b) of the girder web with reinforcement layout (length units: cm; units for bar diameter: mm).
Fig. 15 Longitudinal section of the half joint with reinforcement layout (length units: cm; units for bar diameter: mm).
Fig. 16 Model A for case 1 (length units: cm; units for bar diameter: mm).
Fig. 17 Model A for case 2 (length units: cm; units for bar diameter: mm).
Fig. 18 Model A for case 3 (length units: cm; units for bar diameter: mm).
Fig. 19 Model B (length units: cm; units for bar diameter: mm).
Fig. 20 Model C for case 1 (length units: cm; units for bar diameter: mm).
Fig. 21 Model C for case 2 (length units: cm; units for bar diameter: mm).
Fig. 22 Model C for case 3 (length units: cm; units for bar diameter: mm).

Figure 1

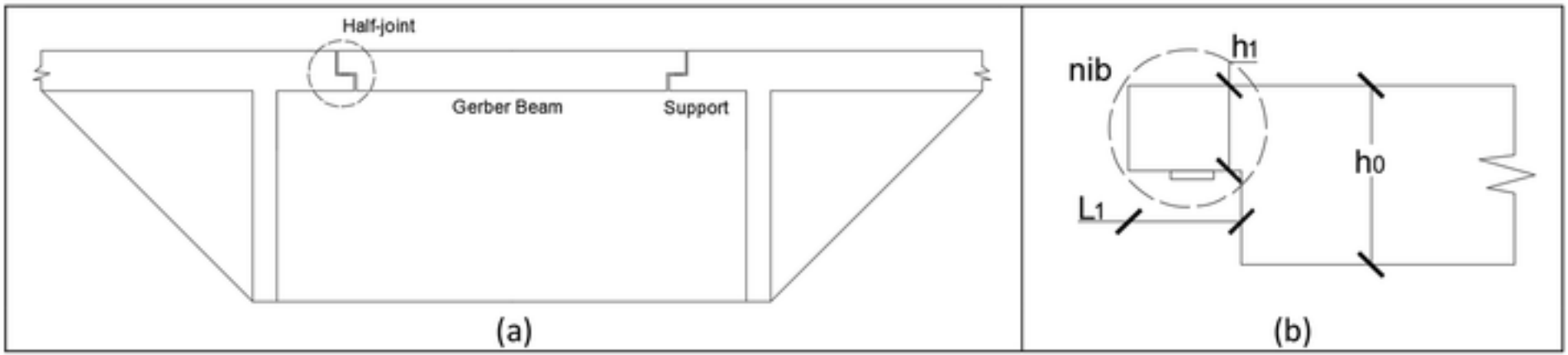

Figure 2

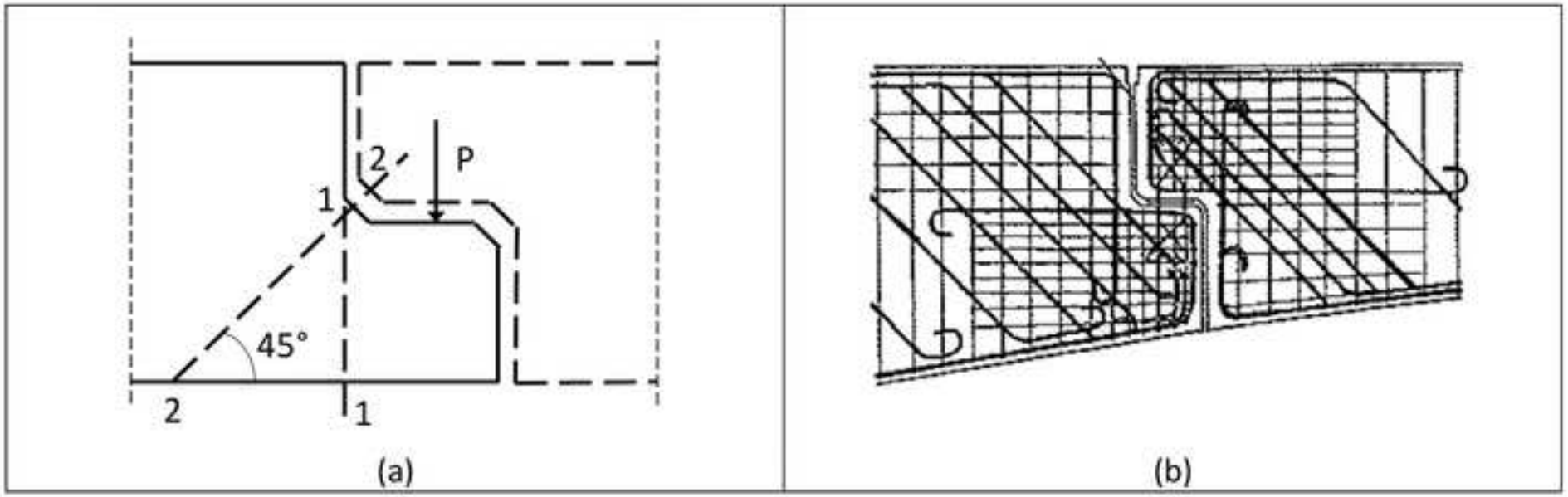

Figure 3

Click here to access/download;Figure;Fig3.tif

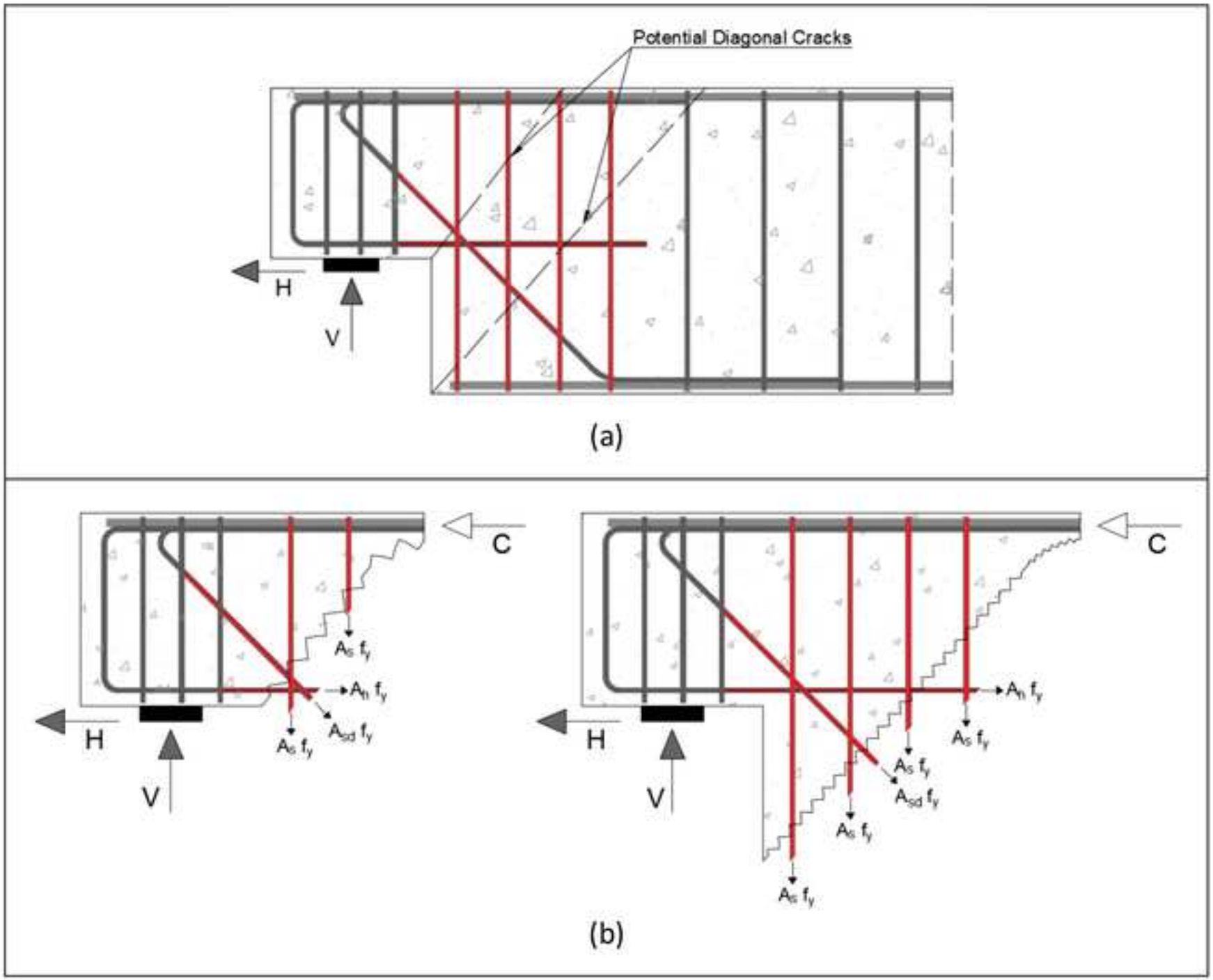

Figure 4

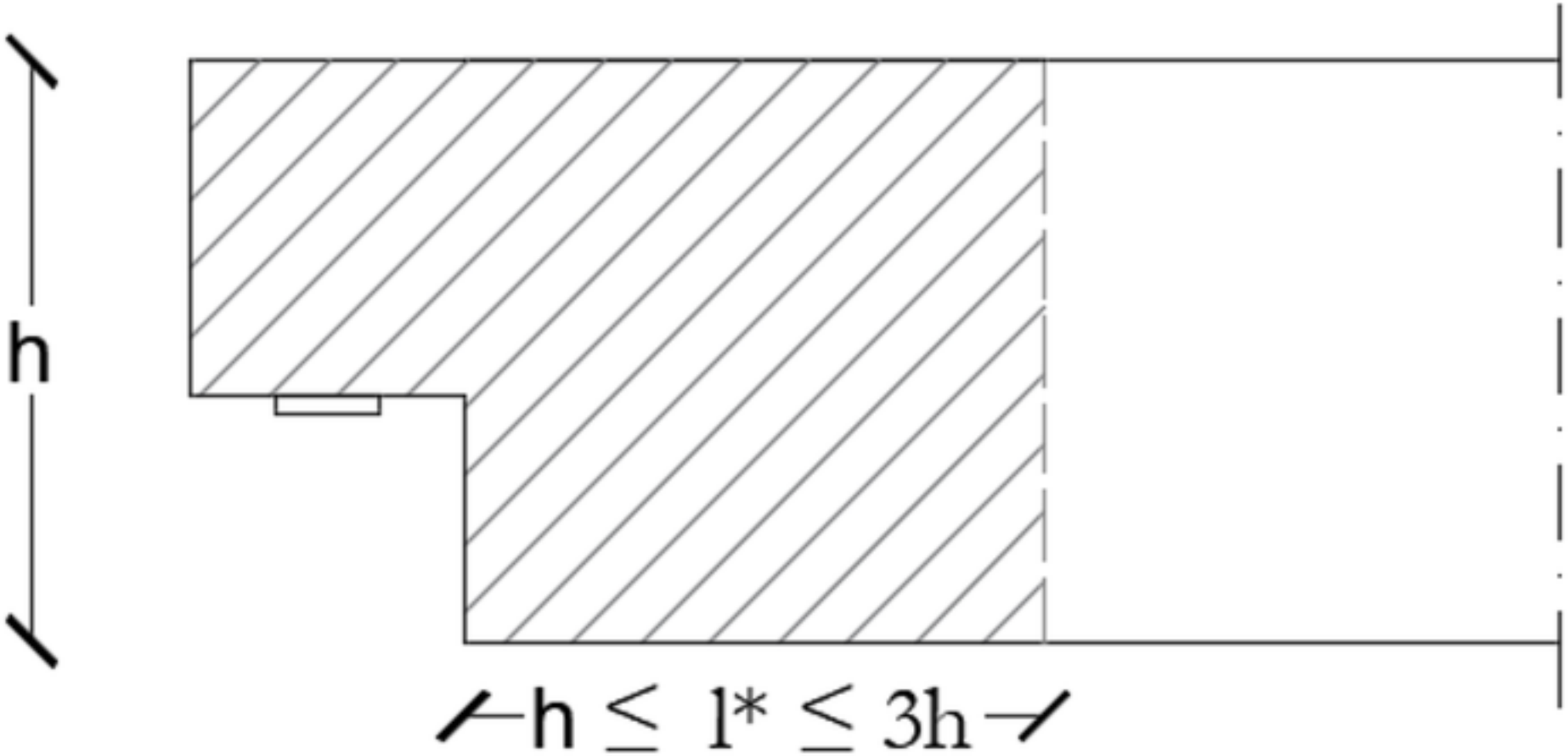

Figure 5

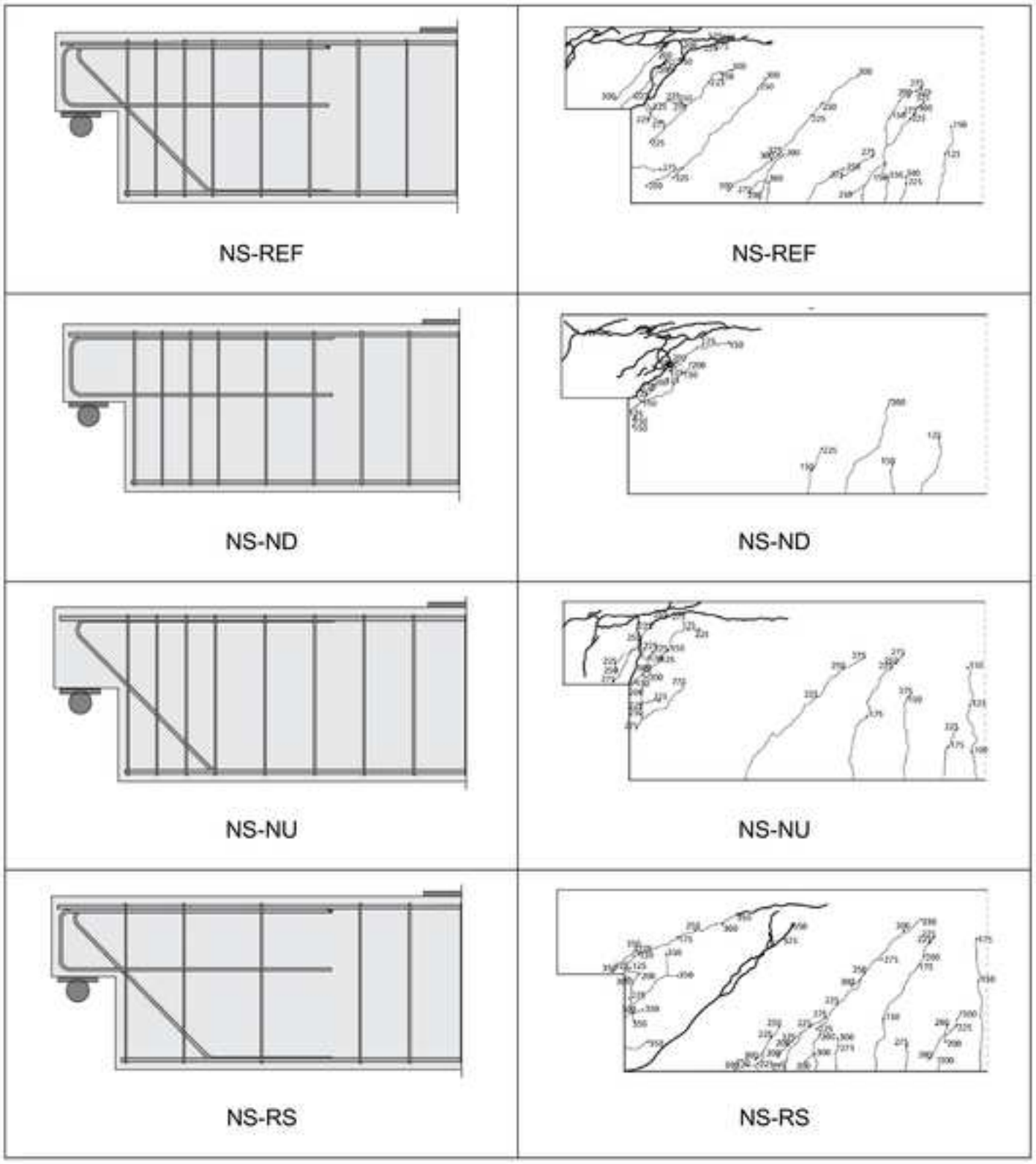

Figure 6

Click here to access/download;Figure;Fig6.tif

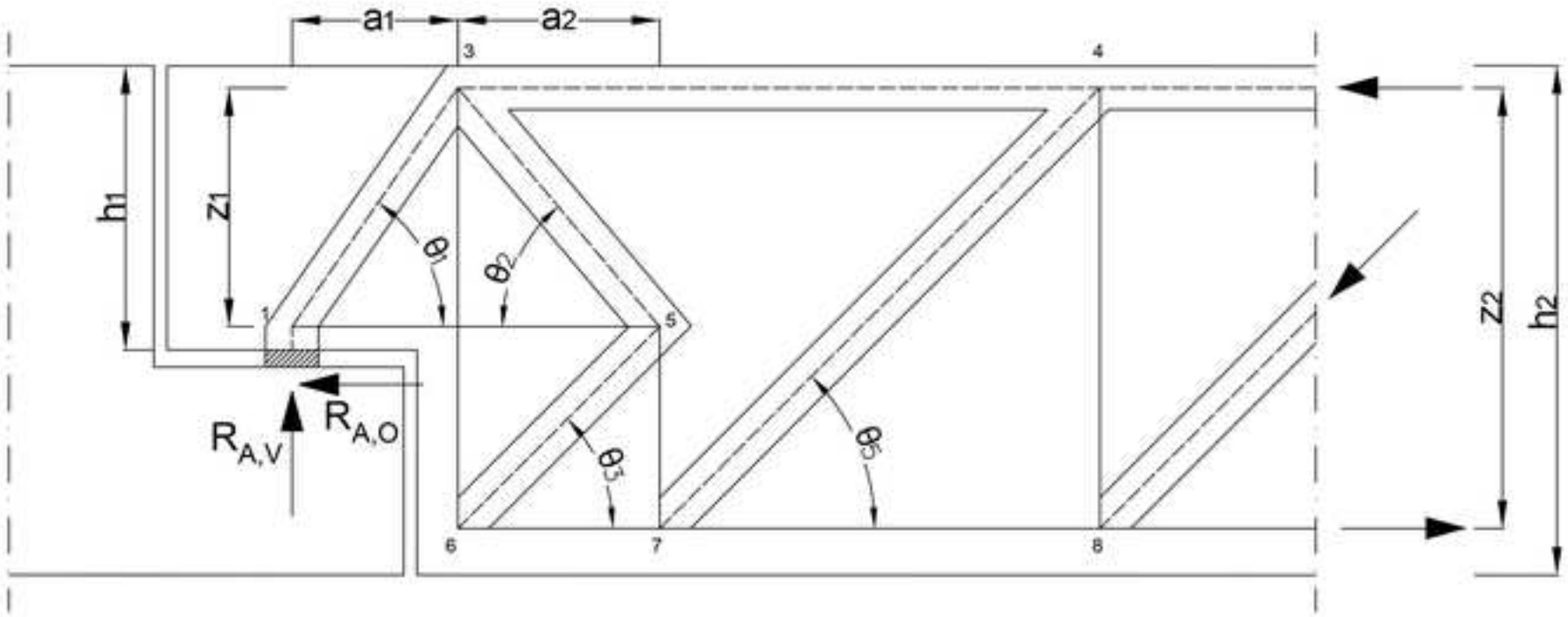

Figure 7

Click here to access/download;Figure;Fig7.tif

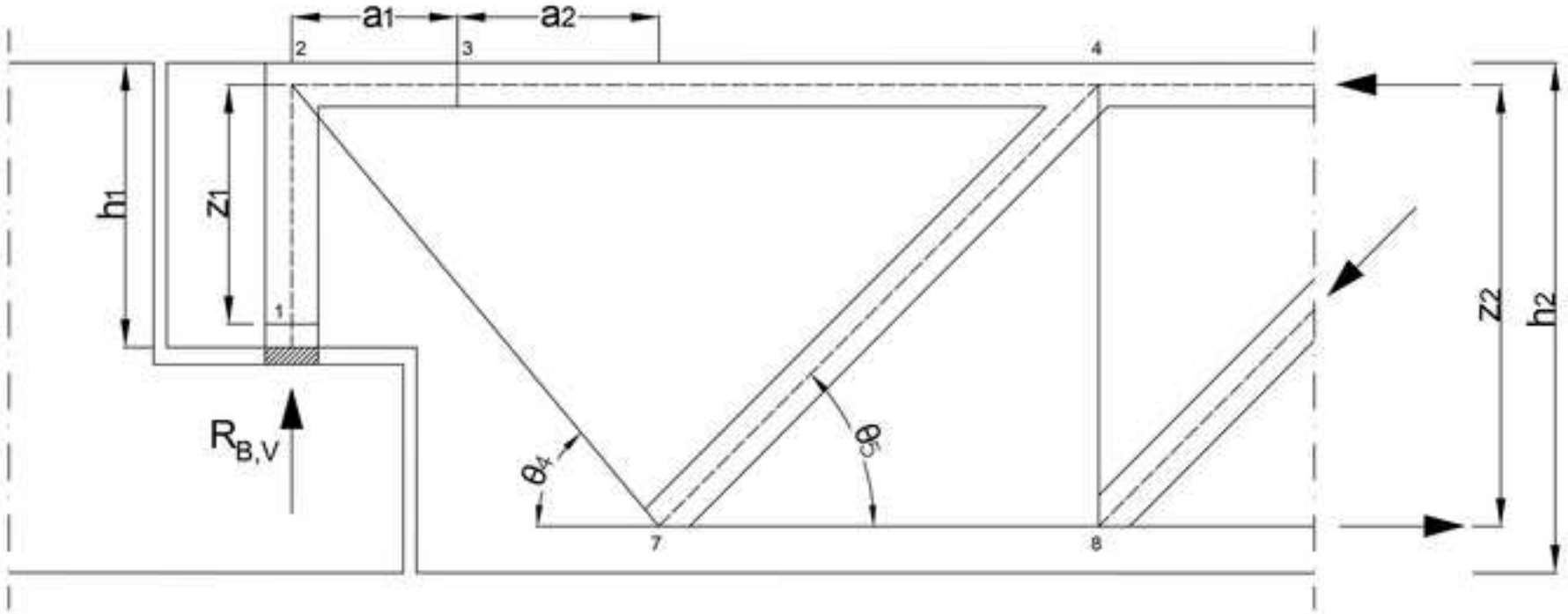

Figure 8

Click here to access/download;Figure;Fig8.tif

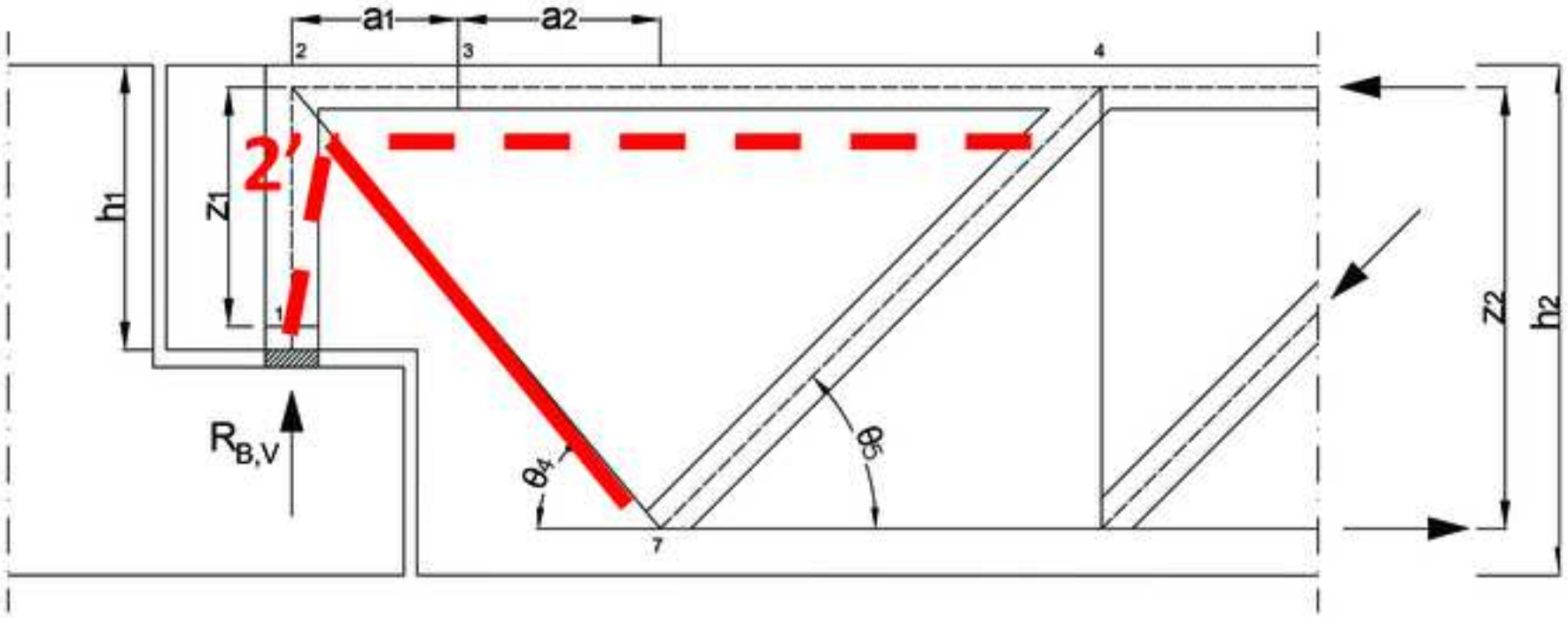

Figure 9

Click here to access/download;Figure;Fig9 v.02.tif

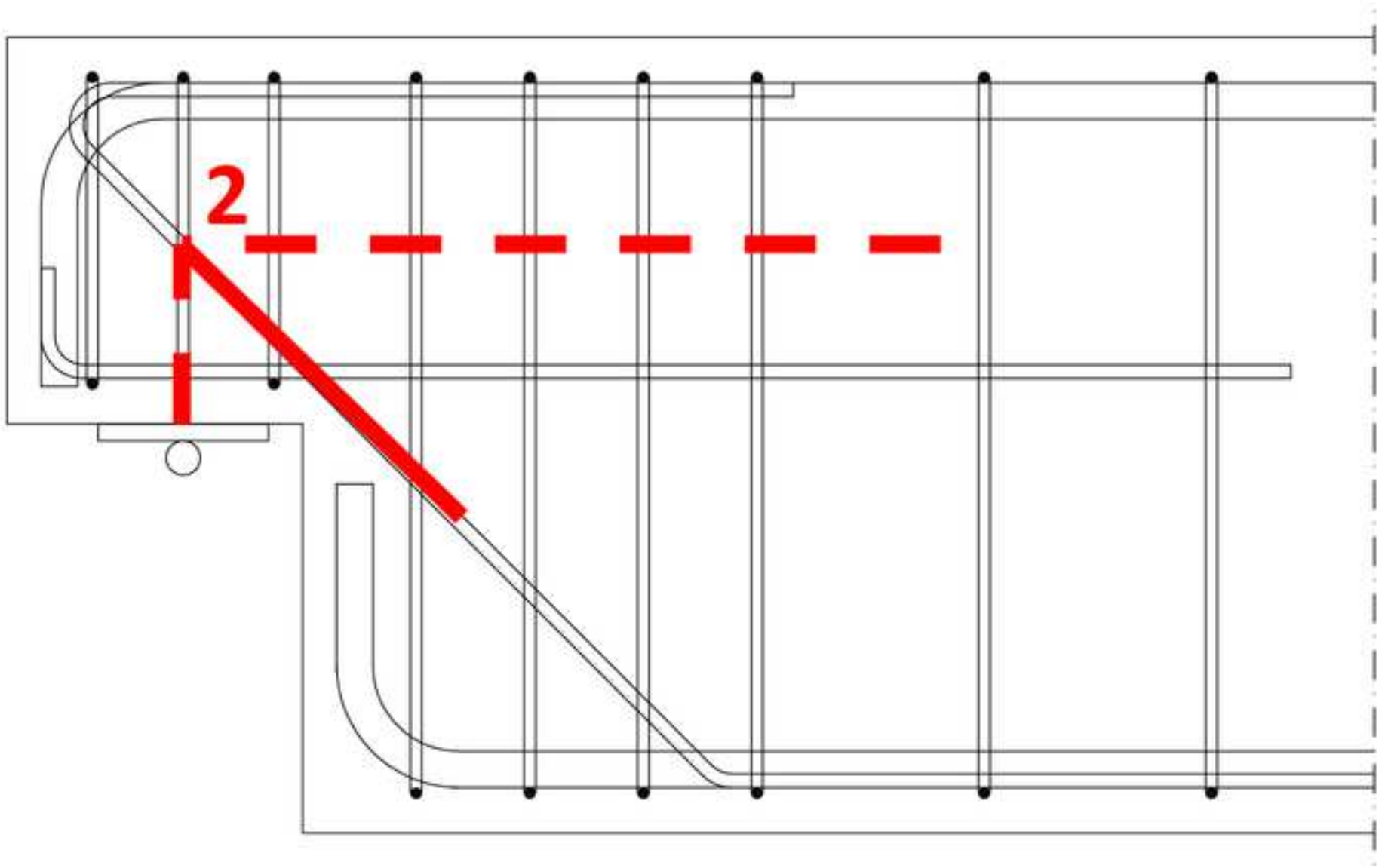

Figure 10

Click here to access/download;Figure;Fig10.tif

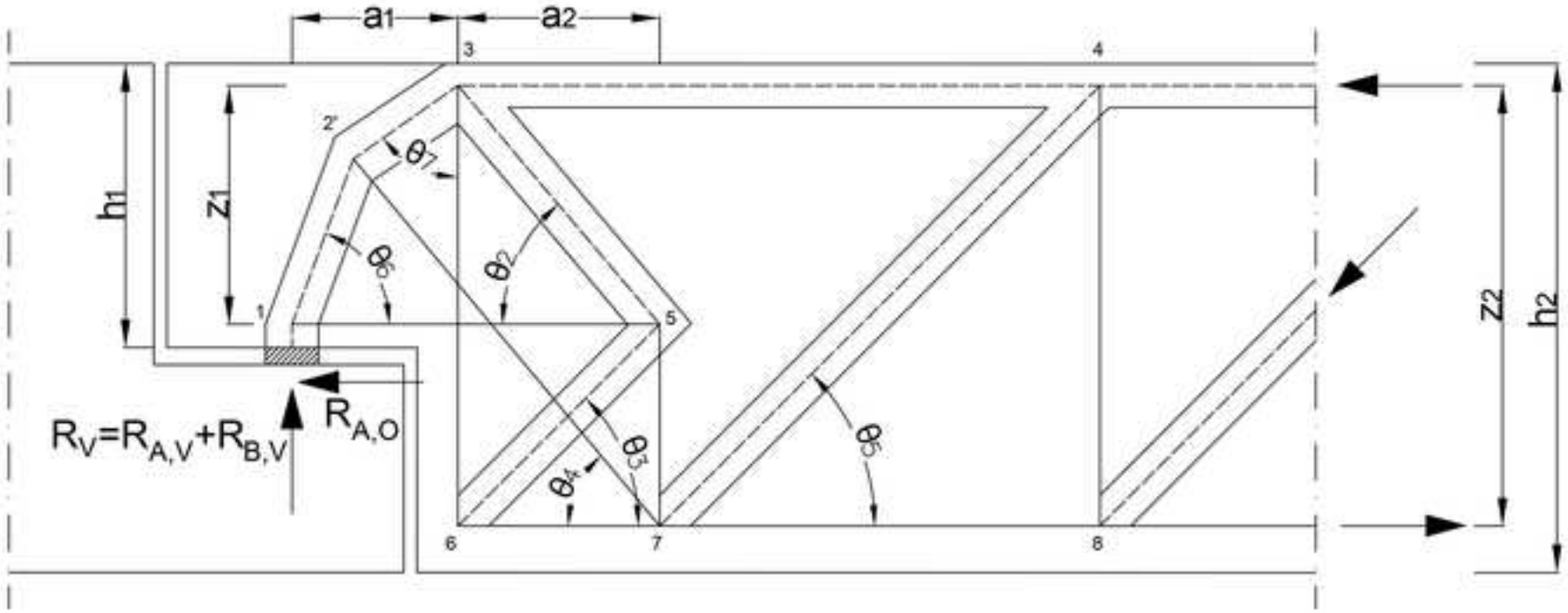

Figure 11

Click here to access/download;Figure;Fig11.tif

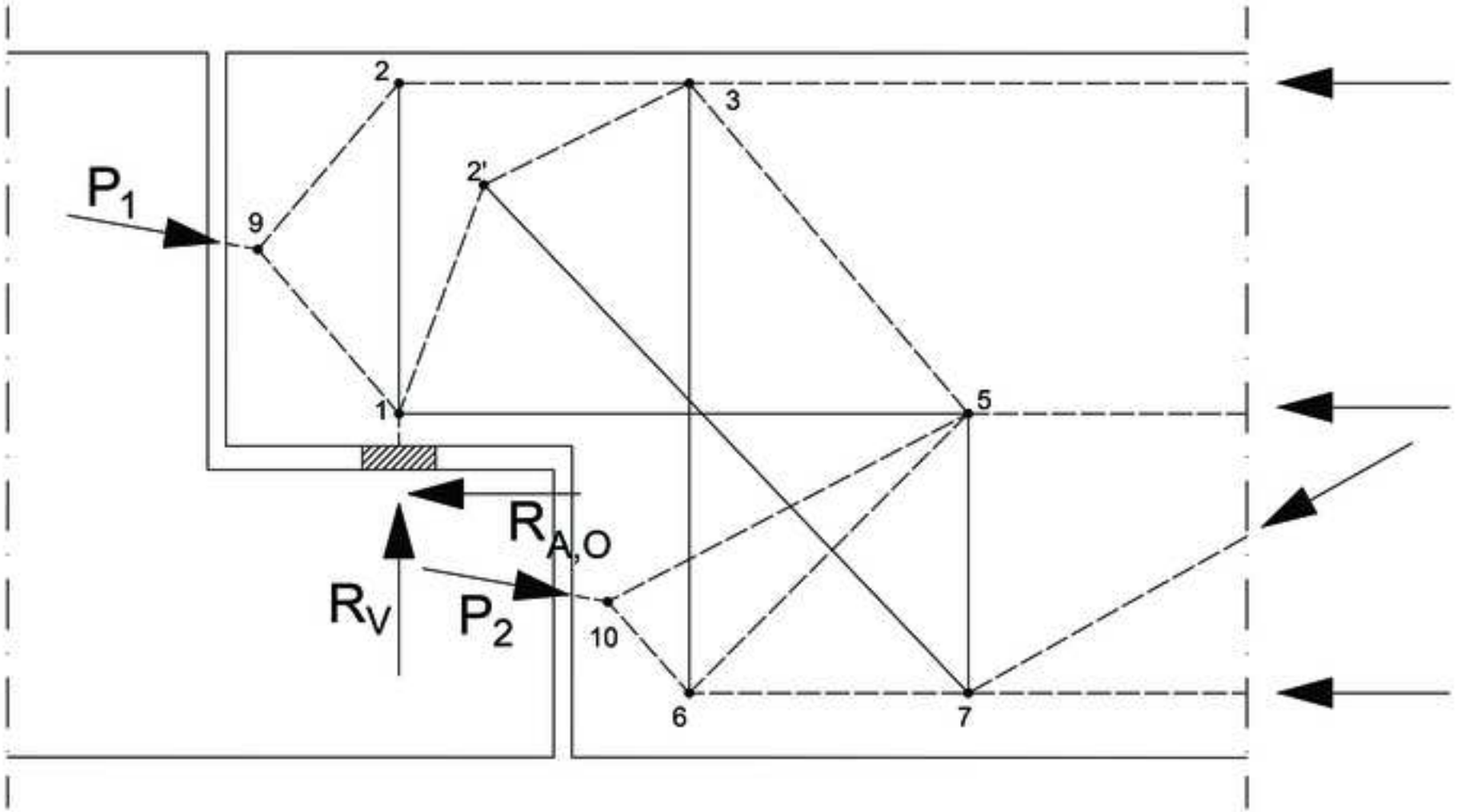

Figure 12

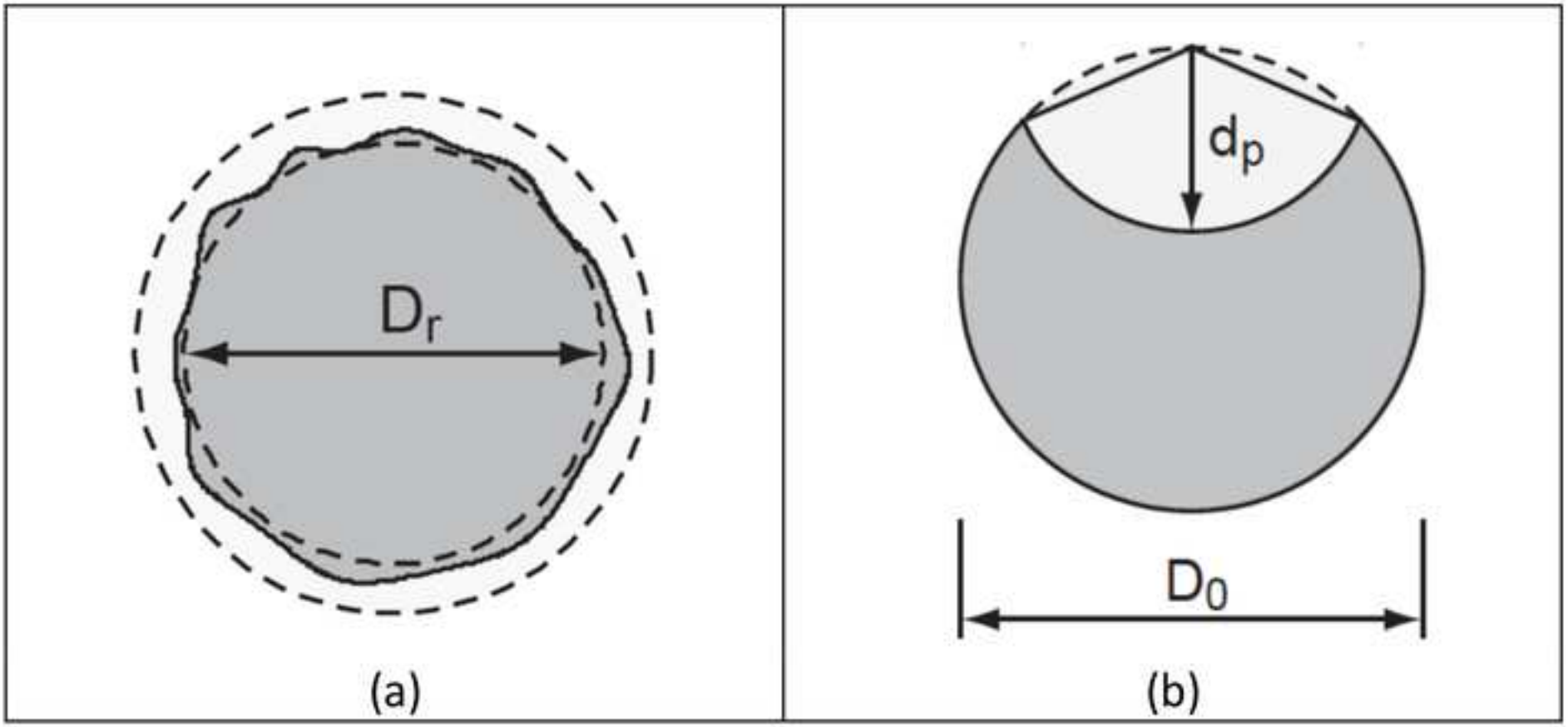

Figure 13

Click here to access/download;Figure;Fig13.tif

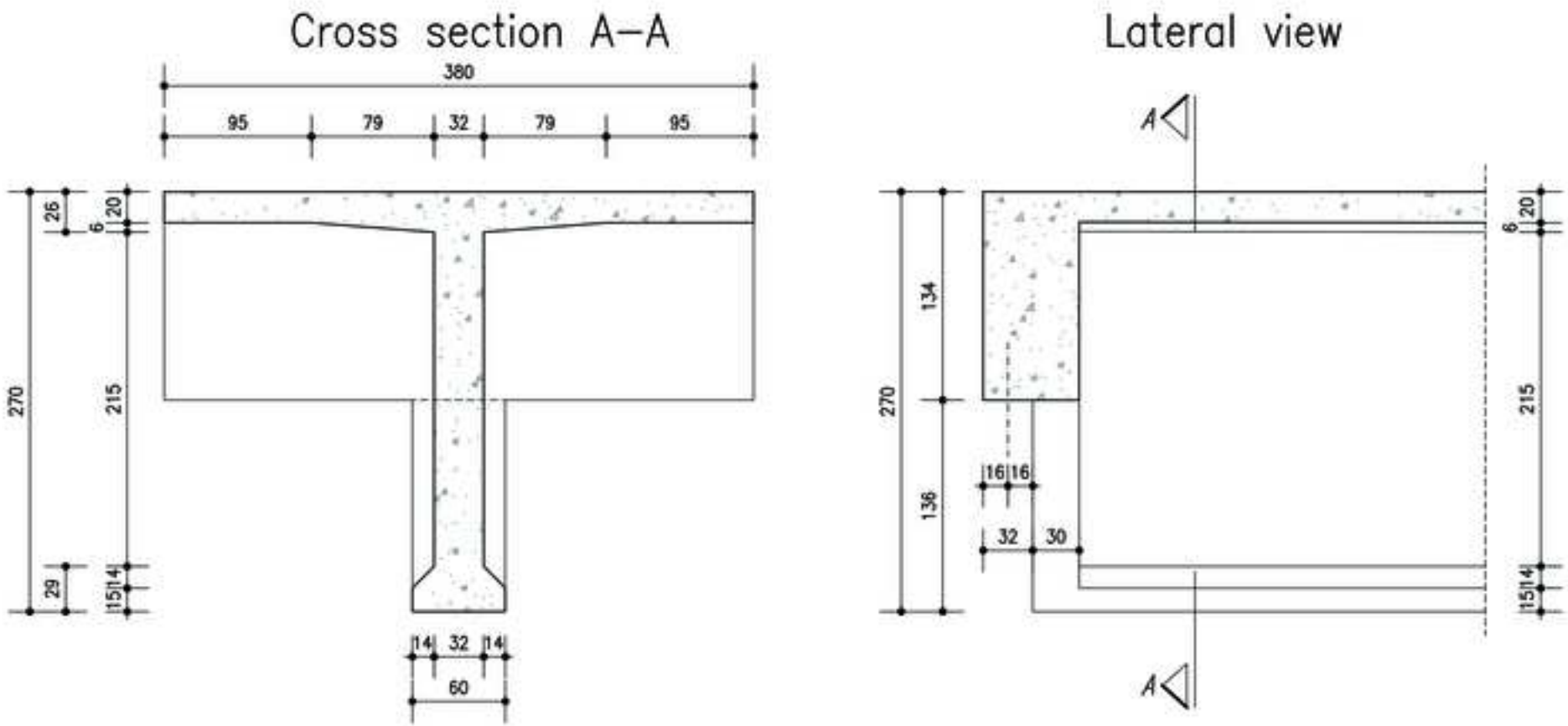

Figure 14

Click here to access/download;Figure;Fig14.tif

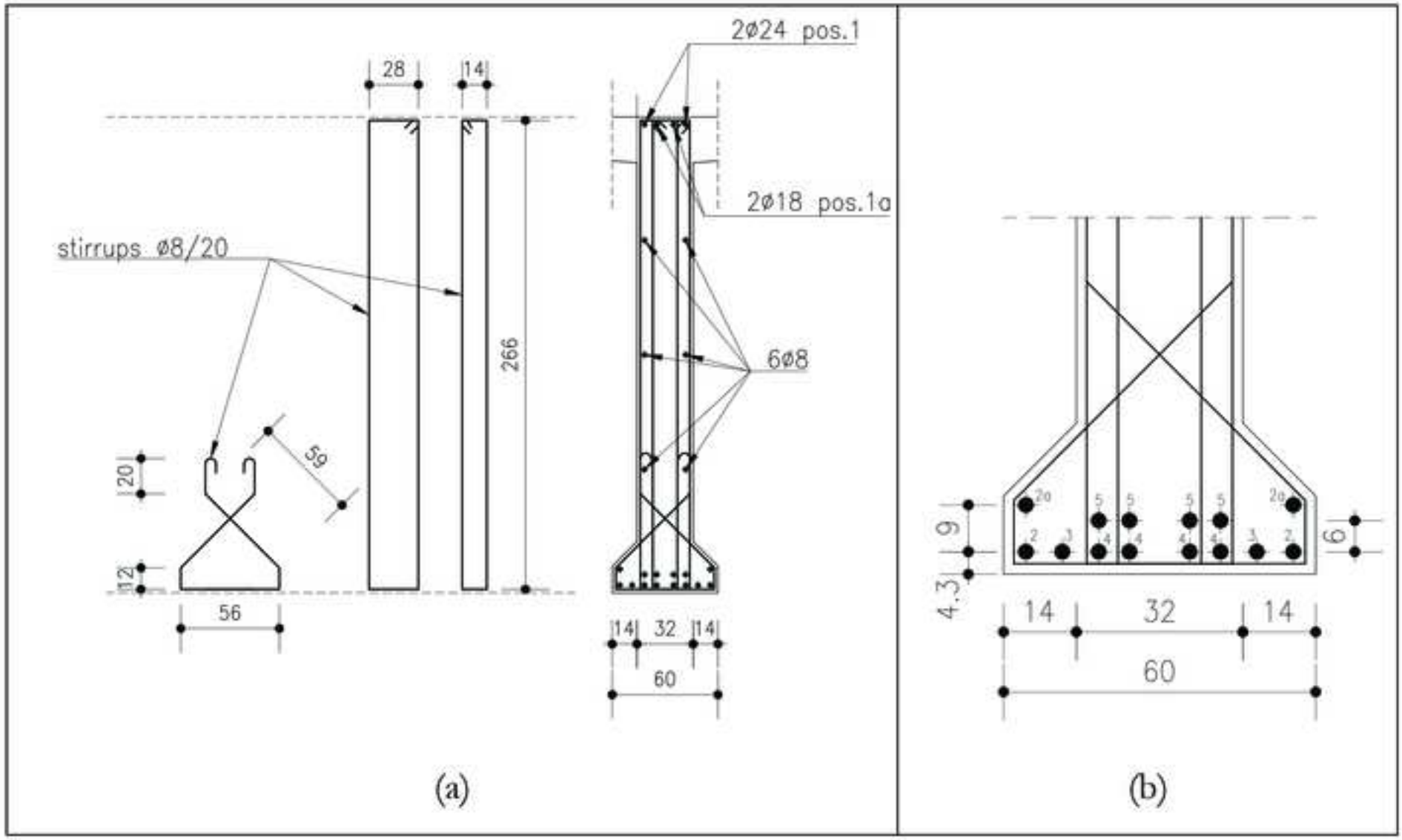

Figure 15

Click here to access/download;Figure;Fig15.tif

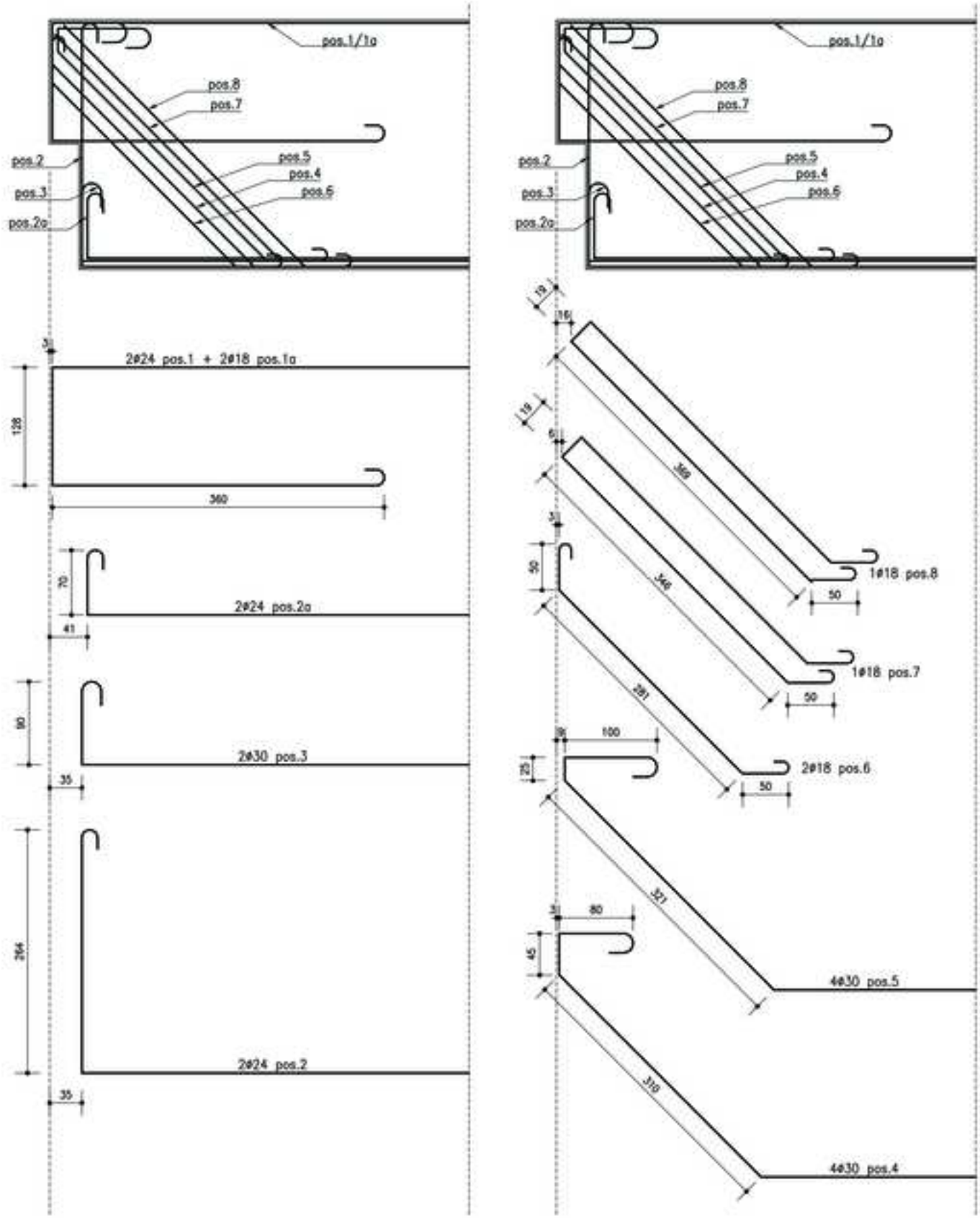

Figure 16

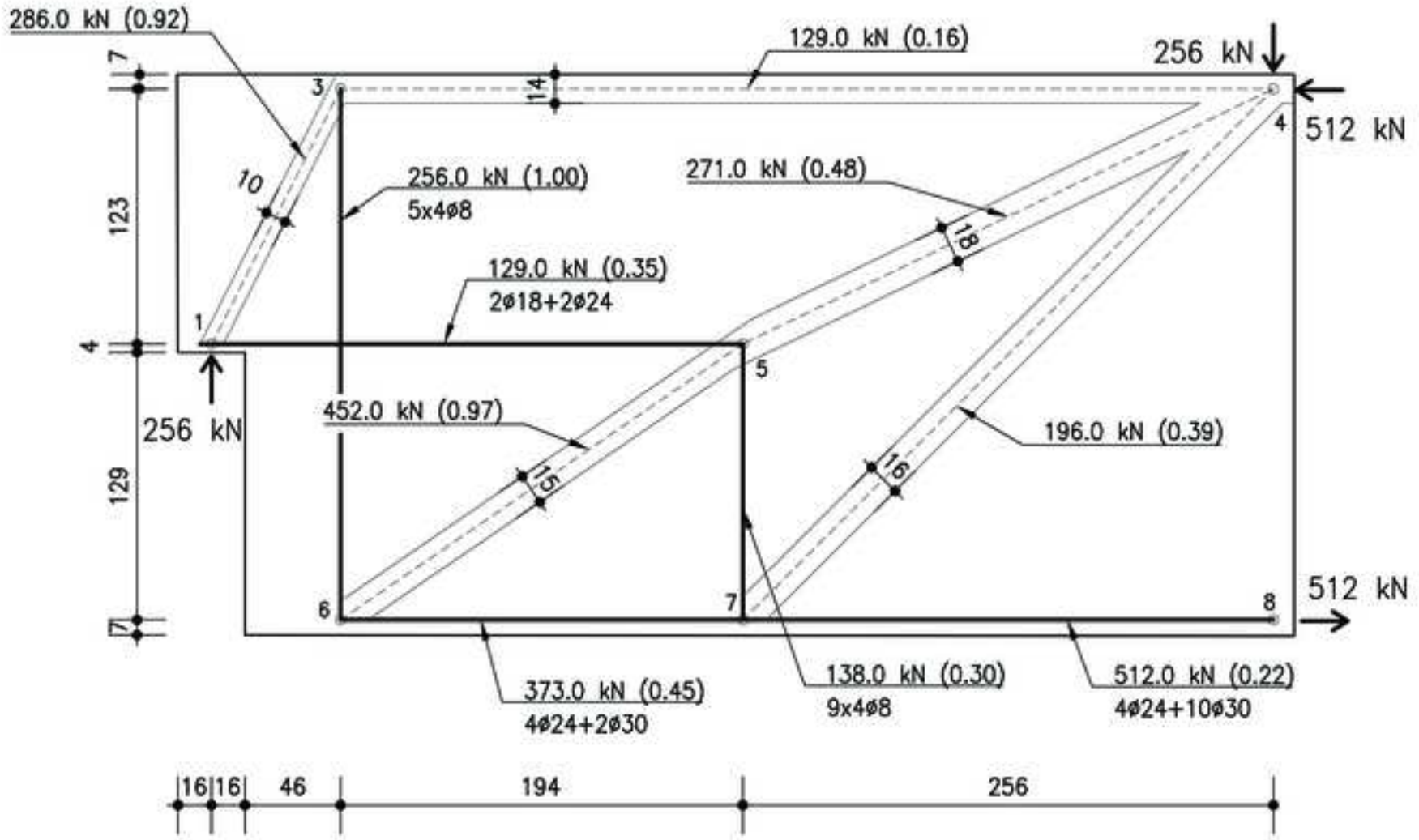

Figure 17

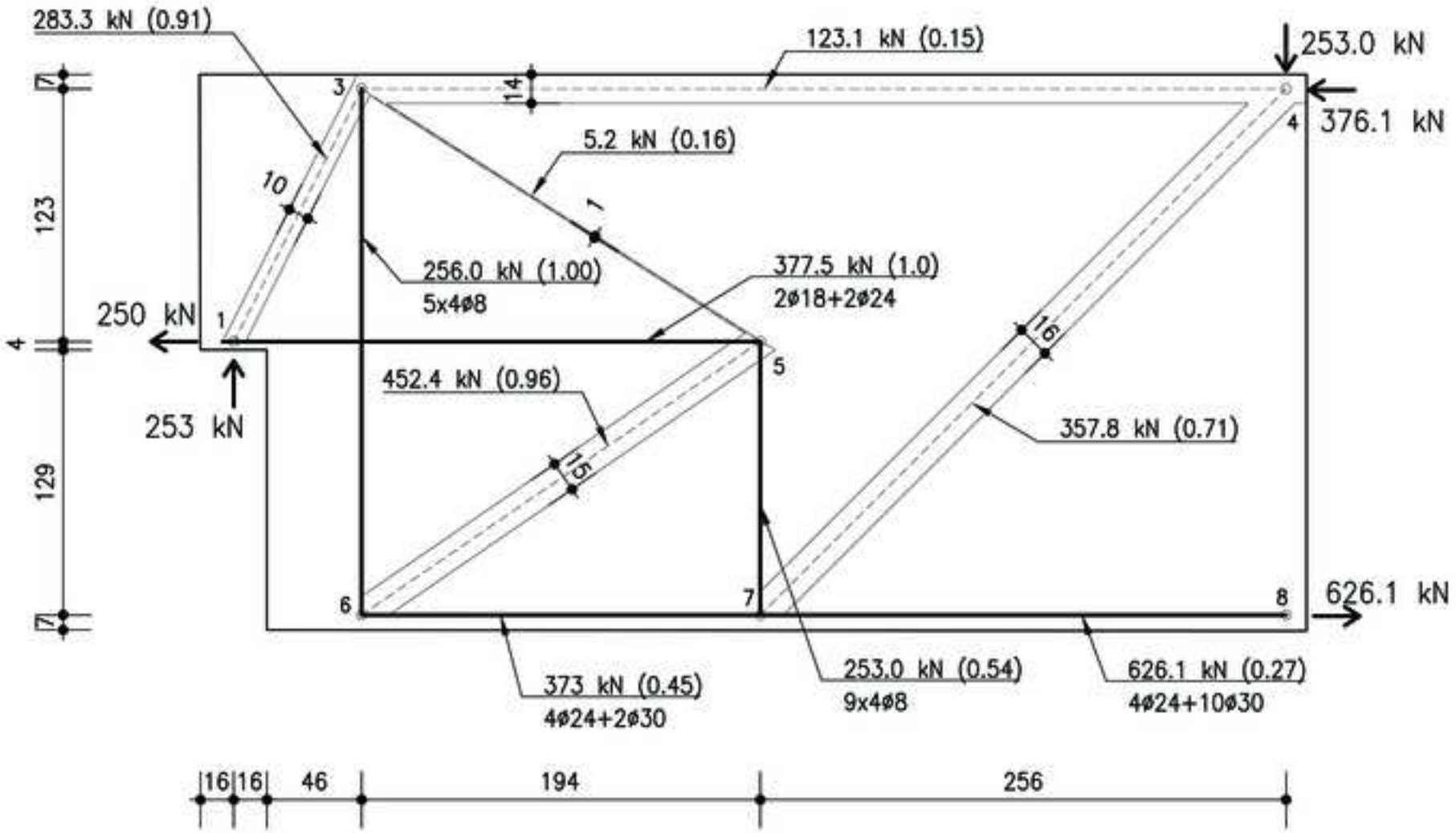

Figure 18

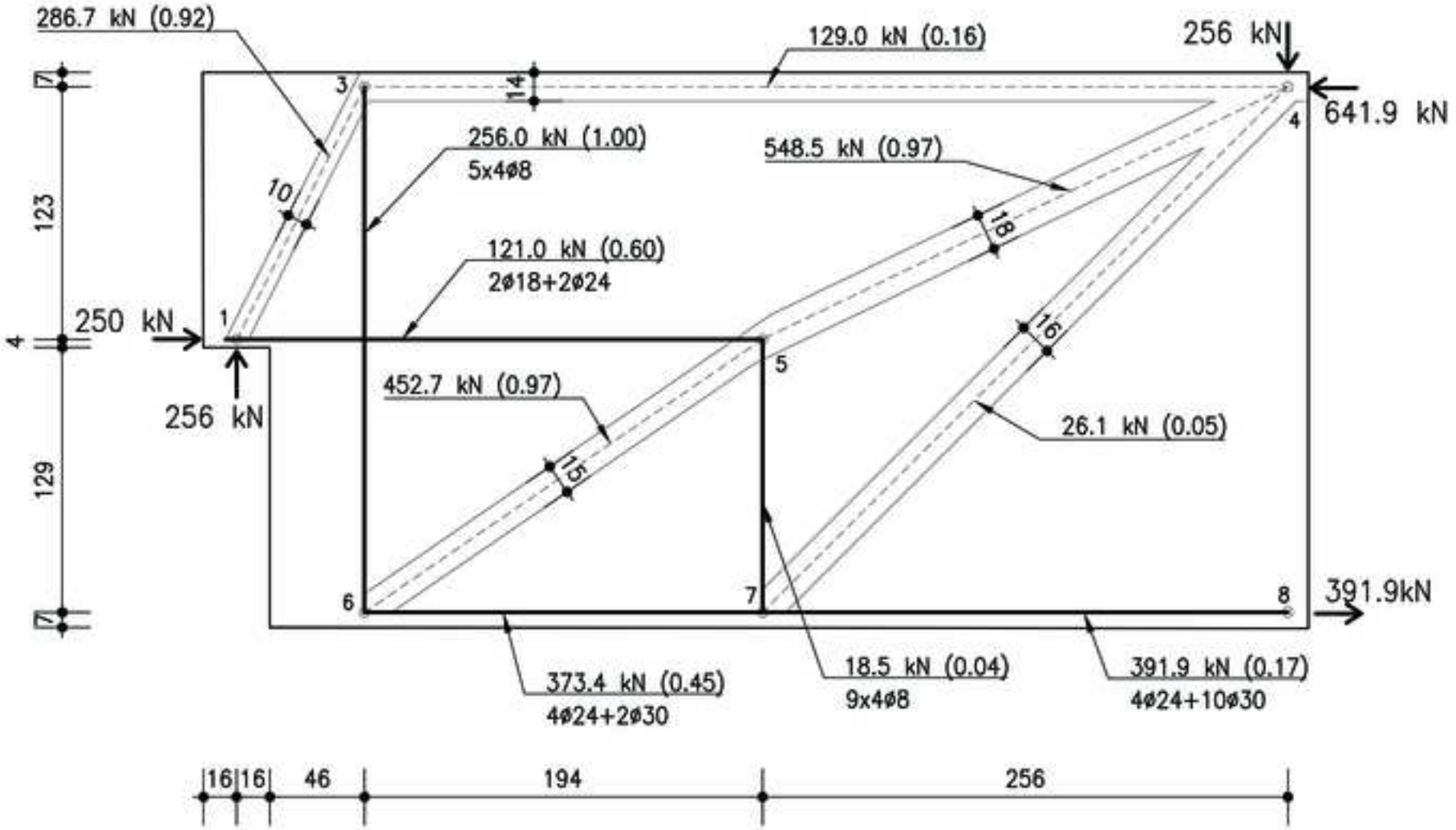

Figure 19

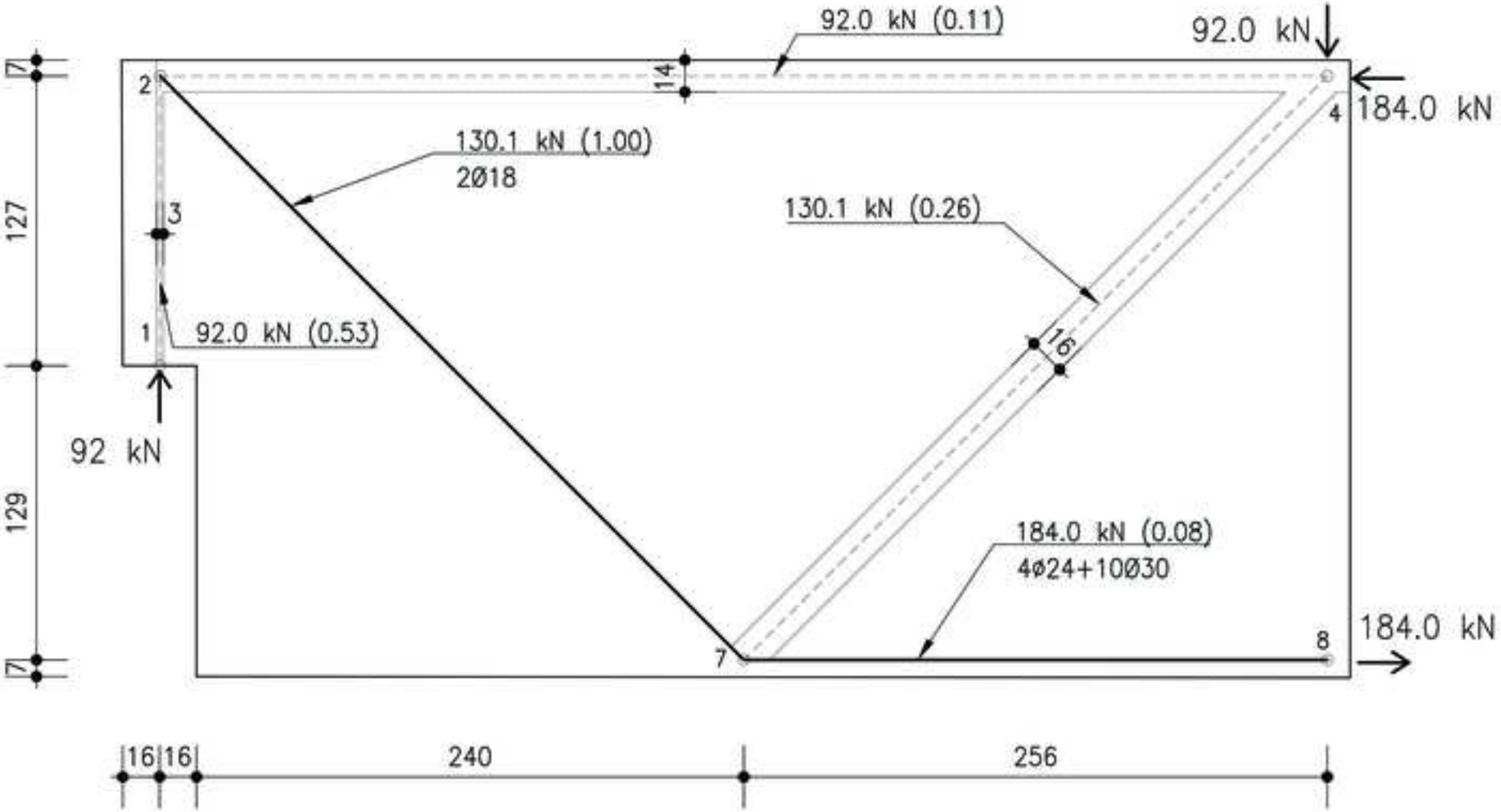

Figure 20

Click here to access/download;Figure;Fig20 v.02.tif

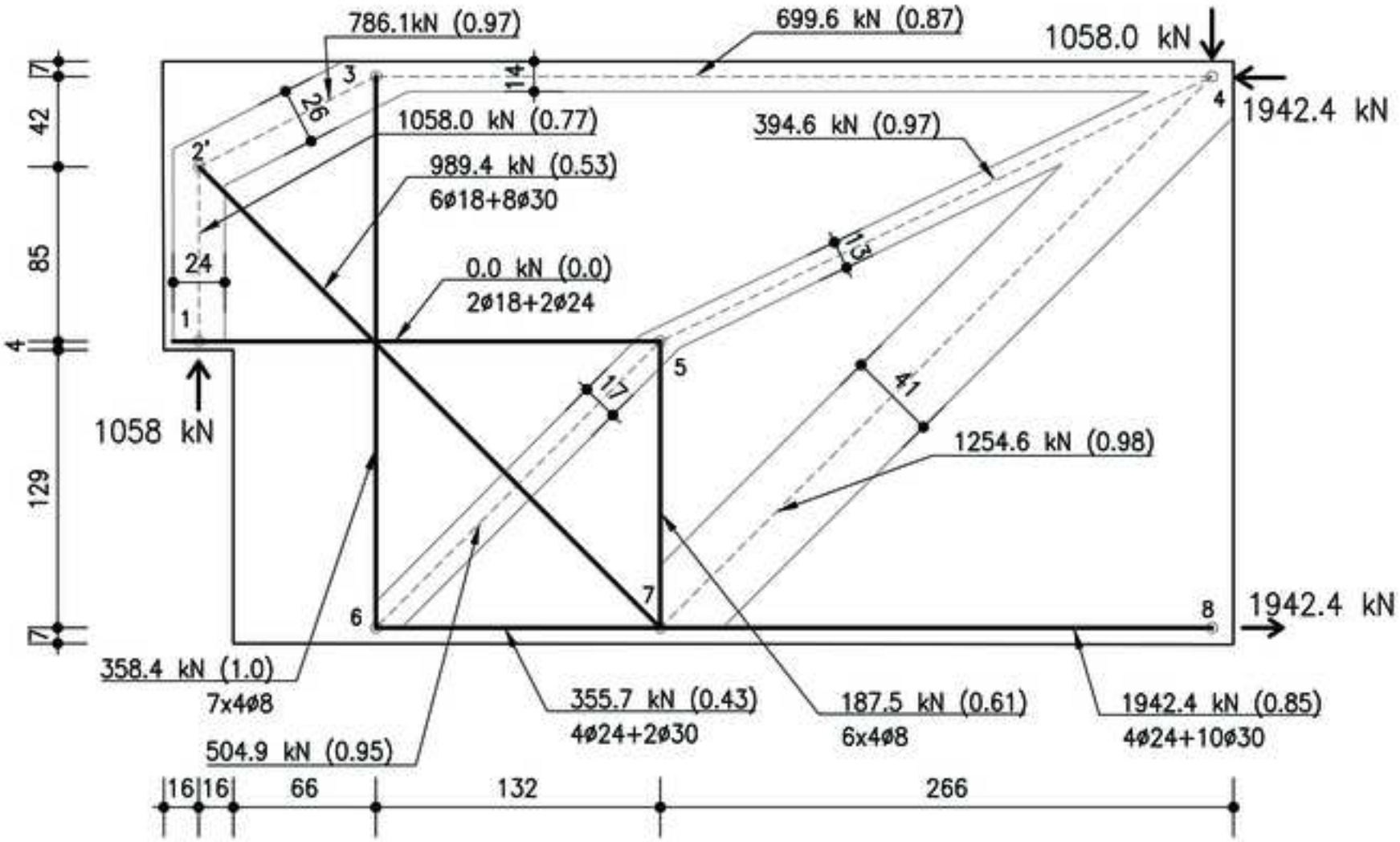

Figure 21

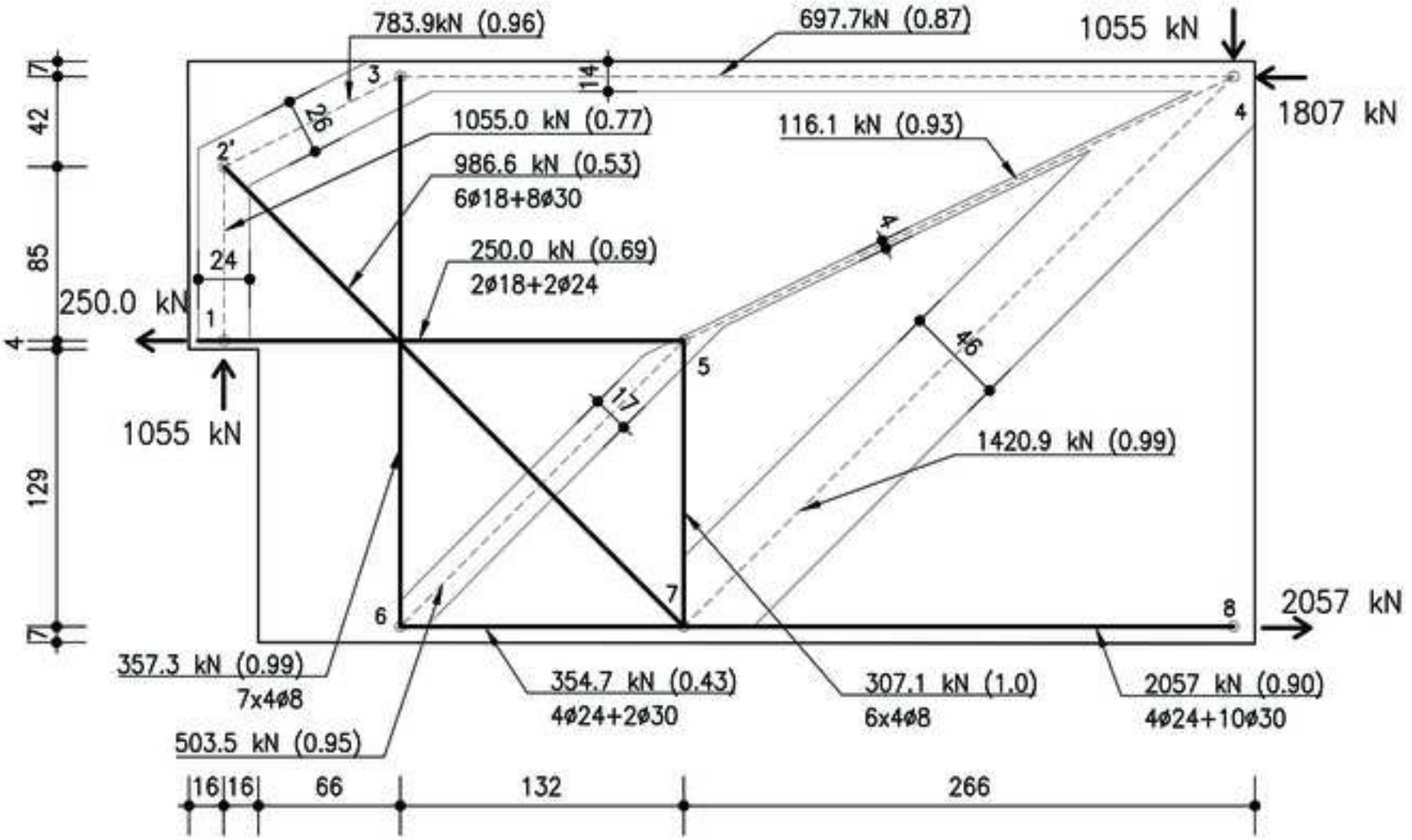

Figure 22

Click here to access/download;Figure;Fig22 v.02.tif